Bart E. Stolk

Design of a steerable introduction shaft for electrode implantation on the dorsal root ganglion

Technische Universiteit Delft

TU Delft Delft University of Technology

Challenge the future

Design of a steerable introduction shaft for electrode implantation on the dorsal root ganglion

By

Bart E. Stolk

in partial fulfilment of the requirements for the degree of

Master of Science
in Mechanical Engineering

at the Delft University of Technology,
to be defended publicly on Tuesday February 26, 2019 at 2:00 PM.

Student number: 4326571

Thesis committee:	Prof. P. Breedveld	TU Delft, supervisor
	Dr. D.H. Plettenburg	TU Delft
	M. Sc. M. Scali	TU Delft, supervisor
	M. Sc. C. Culmone	TU Delft, supervisor

TU Delft Delft University of Technology

Preface

For as long as I can remember, I have been passionate about the cooperation between humans and machines. What started as having my first personal computer as a child, grew to an interest in robots and in prostheses that can be controlled with the human brain. My passion for human-machine interfaces drove me to study a bachelor's and master's degree in mechanical engineering.

When I showed my interest for the human nervous system to professor Paul Breedveld one year ago, he got me in contact with professor Martijn Malessy, an amazing neurosurgeon at the university hospital of Leiden. Martijn gave me the opportunity to follow his working routine for three months to teach me as much about the human nervous system as possible. Besides studying the sensing of peripheral nervous system activity, I joined him in many interesting surgeries ranging from peripheral nerve repair to the removal of brainstem tumors. We talked to patients with all types of neuropathic pain, making me eager to help these patients by applying the knowledge and skills I have gained in the past five years. After doing a literature study on minimally-invasive instruments that can deliver implants into the human body, I decided to design my own implantation instrument. This thesis describes the design of an instrument that helps to implant an electrode lead close to the spinal cord to relieve neuropathic pain and is called: "Design of a steerable introduction shaft for electrode implantation on the dorsal root ganglion". This paper is the final submission for a Master of Science degree in Mechanical Engineering with the Biomechanical Design track, specializing in Bio-inspired Technology at the Delft University of Technology.

I want to thank my supervisors Marta Scali and Costanza Culmone for their continuous help and feedback throughout the course of this project. I want to thank Paul Breedveld and Martijn Malessy for providing me with the freedom to come up with my own project, and for always trying to find time to meet me in their busy schedules. I want to thank doctor Katja Bürger for providing me with conventional electrode implantation techniques and equipment, PhD-student Juan Cuellar for letting me use his 3D-printer, and technician Remi van Starkenburg from DEMO for providing me with his knowledge and skills on building a prototype. Finally, I want to thank my girlfriend, family and friends for their support during this challenging but exciting time. I hope you will enjoy reading this thesis, as I sure have enjoyed writing it.

Bart E. Stolk

Delft, January 2019

Contents

The design of a steerable introduction shaft for electrode implantation on the dorsal root ganglion

Bart E. Stolk

Abstract – Sensory nerve roots (DRGs) that emerge from the spinal cord can be stimulated with electrodes to prevent neuropathic pain. Proper functionality of DRG stimulation strongly depends on electrode placement, and the DRG coverage of the implanted electrode lead is limited with the use of conventional pre-curved introduction shafts. The goal of this thesis is to design an introduction shaft with a steerable tip in one direction to decrease the minimum radius of curvature and increase the angle of curvature of the implanted electrode leads around DRGs. The steerable tip design consists of clamped stainless-steel rings on a nitinol rod and an internal braided stainless-steel pulling cable attached to the distal ring to bend the tip. A handle provides minimum radius of curvature adjustment for different DRG sizes, and combined shaft translation and tip bending for circular motion around the DRG. A scale-up prototype was manufactured, and the tip had an outer diameter of 2.4 mm and a length of 22 mm. A tip bending fatigue test was performed, during which the steerable tip showed no plastic deformation. The steerability of the tip was tested in gelatin and resulted in a DRG circumference coverage of 51.4% ± 1.1% compared to a 25% potential coverage of conventional introduction shafts. The minimum radius of curvature was adjustable between 42 ± 14 mm and 6 ± 1 mm. An electrode lead was successfully implanted in an artificial environment that mimicked a section of the spine. In the future, the outer diameter of the prototype tip should be decreased to reach the required size for the procedure (1.6 mm), and the handle should contain a mechanism to increase shaft translation relative to the tip bending in order to improve circular motion of the steerable tip.

1 Introduction

1.1 Electrode implantation on the dorsal root ganglion

The peripheral nervous system is the connection between the central nervous system and the rest of the body. It consists of sensory and motor nerves that emerge from the spinal cord and come together in the intervertebral foramen, the space in between vertebrae. Sensory nerves transmit signals like pain, temperature, and proprioceptive inputs to the central nervous system. The cell bodies of sensory nerves are located together in a spherical-shaped nerve root in the intervertebral foramen called the dorsal root ganglion (DRG). Humans have 31 pairs of DRGs emerging from the spinal cord, one pair in between each spinal vertebra next to the spinal cord [1-3] (Figure 1a). Motor nerves and the DRG are encapsulated with the spinal cord inside the intervertebral foramen by a protective sheath called the dura (mater), and the dura is protected further by a fat-filled epidural space in between the spinous processes and the vertebrae (Figure 1b-d).

If a peripheral nerve is damaged, the lesion site on the nerve fiber of a damaged sensory nerve starts to generate electrical stimuli. These stimuli are often followed by stimuli of the cell bodies of the damaged sensory nerves in the DRG and can result in the perception of pain [4]. This progressive chronic nervous system disease is called neuropathic pain and affects an estimated 6-8% of the global population [5]. To suppress neuropathic pain, an electrode lead can be placed on the dura around the DRG. Electrodes are metal conductors, and an electrode lead is a flexible plastic shaft with an electrode array on each end of the lead (Figure 2). Electrode arrays consist of equally spaced electrodes and are connected via internal cables in the lead shaft. One end of the lead is connected to a pulse generator to produce an electrical signal on the other end of the lead, which interacts with the DRG to achieve pulsed depolarization of the nerves [6]. Depolarization of the damaged nerves diminishes the generated stimuli of the DRG to relieve neuropathic pain. Proper functionality of DRG neurostimulation strongly depends on the accuracy and precision of the electrode

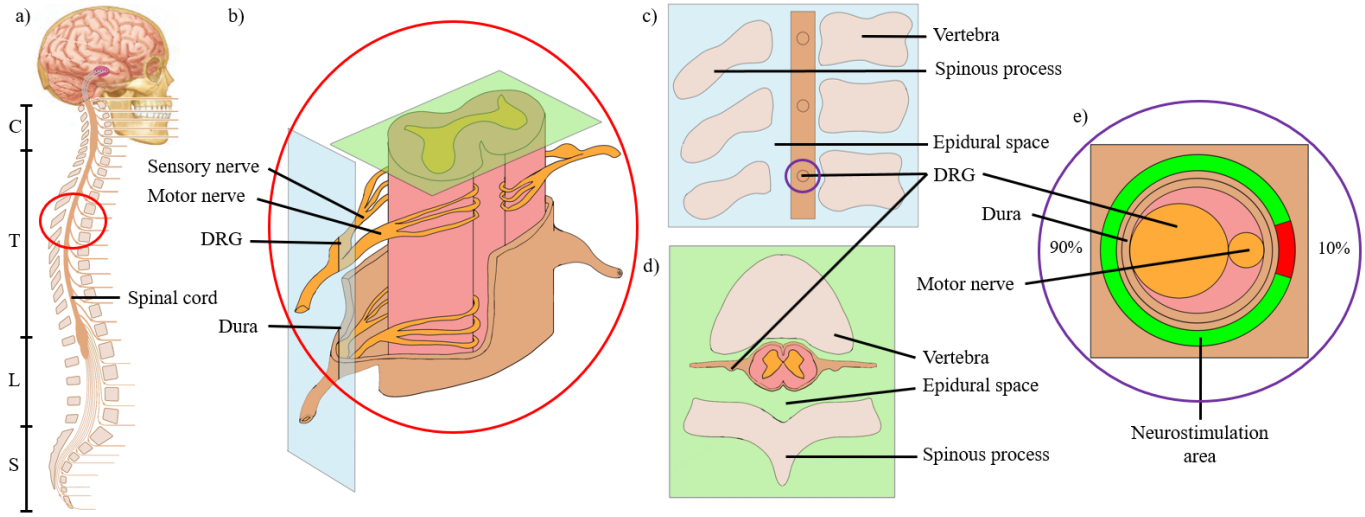

Figure 1. Central nervous system and the peripheral nerves that emerge from the spinal cord (a) (Source: Adapted from [1]). The C, T, L and S (left) are abbreviations for the cervical, thoracic, lumbar and sacral spinal regions respectively. A part of the spinal cord (b), a lateral/sagittal view of the spine and the spinal cord (c), a top/transverse view of the spine and the spinal cord (d), and a lateral/sagittal view of the nerves that emerge from the spinal cord with a circle around the dura to show desirable DRG stimulation (green) and undesirable motor nerve stimulation (red) (e).

implantation. An inaccurate position of the electrodes is the cause of failure of neurostimulation in one out of three patients and can leave patients with tedious side-effects [6].

In DRG electrode implantation, the dura is not pierced or locally removed to prevent damage to the sensory and motor nerves. The DRG can therefore not be stimulated directly, as the dura is located in between the DRG and the electrodes, and the DRG cannot be fully surrounded by electrodes without undesirable stimulation of motor nerves (Figure 1e). Stimulation of motor nerves can be unpleasant for patients, but motor nerves only take up a small percentage (about 10% according to neurosurgeon M.J.A. Malessy) of the surface area of the dura around a DRG and its correspondent motor nerve [7]. Lumbar and sacral DRGs have a spherical shape with a width of 2-8 mm and a length of 3-15 mm and have different dimensions depending on the spinal region [8-11]. Ideally, electrode leads are implanted in a full circle around the DRG to cover the whole circumference of the DRG, as individual electrodes on the electrode array on the electrode lead can be switched off to prevent motor nerve stimulation. However, electrodes are currently implanted around a limited part of the DRG to prevent motor nerve stimulation and because of limited implantation maneuverability during the implantation procedure.

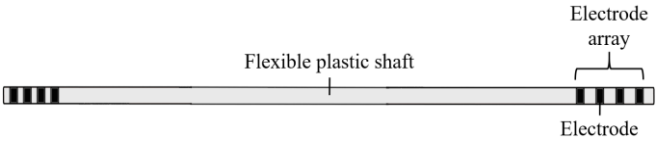

Figure 2. Electrode lead with an electrode array on each side. The arrays are connected via internal cables in the flexible plastic shaft.

1.2 Conventional dorsal root ganglion electrode implantation

This thesis is based on one of the most widely adopted DRG electrode implantation procedures where an electrode lead is implanted around the dorsal part of the DRG [12]. This implantation procedure is henceforth described as the conventional procedure. The conventional procedure is described in steps in Figure 3. In the conventional procedure, an electrode lead (Figure 4a) is implanted with a Tuohy needle (Figure 4c) in the back to reach the epidural space using an introduction shaft (Figure 4b) inside the needle to reach the DRG. The required instruments for the conventional implantation procedure such as the needle, introduction shaft and electrode lead are provided by the Cardiva Group in the AXIUM package [13] (Cardiva, Madrid, Comunidad de Madrid, ES).

Preparation step 1: Choice of the radius of curvature of the introduction shaft tip. To properly stimulate a DRG, electrodes should be implanted as close to the DRG as possible and cover most of the DRG surface area. Lumbar and sacral DRGs (Figure 1a) have a spherical shape with different dimensions depending on the spinal region [11]. To compensate for the spherical shape of DRGs, electrodes are implanted through a plastic introduction shaft with a pre-curved non-steerable tip. The tip is called pre-curved, as the curve in the shaft is applied by the manufacturer and is not meant to change during the implantation procedure. To compensate for different DRG sizes, introduction shaft tips are available with two different radii of curvature. The pre-curved shafts are 220 mm long and have tips with a radius of curvature of about 15 mm and 20 mm [13] (Figure 4a). The pre-curved introduction shaft is chosen with a 15 mm or 20 mm radius of curvature to implant the electrode lead around a relatively small or large DRG respectively.

Preparation step 2: Insertion of the electrode lead into the introduction shaft. The electrode lead is 500 mm long and has two electrode arrays that consist of four electrodes each on both ends of the lead (Figure 4b). Both electrode arrays have different lengths. The largest array has a total length of 20 mm [12] and is called the distal array, as this array is to be implanted around the DRG. The electrodes on the distal electrode array are connected to a shorter proximal electrode array via internal cables in the lead shaft. The proximal electrode array can be attached to the pulse generator to stimulate the distal electrodes. The electrode lead has an inner lumen through which a nitinol rod can be inserted to increase the stiffness of the lead. The electrode lead with the nitinol rod inside is fed through the introduction shaft from the proximal end until the distal end, as the distal array on the lead should be covered completely by the pre-curved introduction shaft tip. The electrode lead can then be locked to the introduction shaft with a leak-free fluid fitting (Luer lock) on the proximal end of the introduction shaft. The outer diameter of commonly used electrodes and the corresponding electrode lead is 1.0 mm. The inner diameter of the introduction shaft is 1.1 mm to allow for sliding of the electrode lead inside the introduction shaft.

Procedure step 1: Insertion of a Tuohy needle into the epidural space. To start the surgery, an incision is made in the back with a scalpel a few centimeters lateral to the spinal cord. A 14-G (2.1 mm outer diameter, 1.7 mm inner diameter) Tuohy needle is then inserted at a 30° angle from the transverse plane and a 30° angle from the coronal plane to pierce through soft tissue in between the spinous processes and reach the epidural space on the dorsal side of the spinal cord. The needle is 115 mm long [14] and has a sharp tip to pierce through soft tissue in between the back and the epidural space. A stainless-steel guide-wire can be inserted into the needle to verify if the epidural space is reached by checking pushing resistance on the guide-wire, as less force is required to push through the fat in the epidural space compared to the tissue in between the spinous processes.

Procedure step 2: Insertion of the introduction shaft through the needle. The introduction shaft with the electrode lead inside is inserted into the proximal end of the Tuohy needle handle while the needle is kept in place. The tip of the needle has a bevel angle of about 8° to 25° [15, 16] (Figure 4c) to allow for a vertical entry of the introduction shaft into the epidural space. The translational motion of the introduction shaft out of the distal end of the needle through the epidural space is monitored with fluoroscopic guidance as the shaft tip is positioned as close to the dorsal area (Figure 5) of the DRG as possible. Both the needle and the introduction shaft have a rectangular shaped handle to allow for rotation. The introduction shafts are made from a relatively flexible plastic (PFA or PEEK) to allow for the angled entry through the needle tip with the bevel angle. The introduction shafts are internally reinforced with stainless-steel braiding to provide enough stiffness to push through fat-filled epidural space [14]. The electrode lead can either be implanted around the closest DRG from the needle tip in the cranial direction (one-level technique) or on the DRG that lies one vertebral level further (two-level technique). This thesis focuses on the two-level technique, as this is used to avoid sharp angles in the introduction shaft during the procedure. DRGs are positioned up to 50 mm laterally from the axis of the spinal cord and up

to 80 mm relatively to the end of the inserted needle tip [8]. The introduction shafts have a slightly smaller outer diameter (1.6 mm) than the inner diameter of the needle (1.7 mm) to allow for sliding inside the needle.

Procedure step 3: Positioning of the introduction shaft tip around the DRG. The introduction shaft with the electrode lead inside is advanced through the needle to surround most of the DRG circumference as possible. This step is the most challenging as the surgeon should position the pre-curved tip around the spherical DRG with only rotation and translation of the introduction shaft relative to the needle. A proper tip position is reached when the tip curvature surrounds the dorsal part of the dura around the DRG and the motor nerve. The dura is not removed or pierced to prevent nerve damage. The electrode lead can be connected to the neurostimulator to stimulate the DRG and verify correct electrode placement. The maximum potential DRG circumference coverage with the pre-curved introduction shafts is around 25%, as the maximum angle of curvature of the shafts is 90˚, which is a quarter of a full circle.

Procedure step 4: Retraction of the introduction shaft through the needle while leaving the electrode lead in place. The Luer lock on the introduction shaft is first disengaged if the electrode lead is locked to the introduction shaft in the second preparation step. The nitinol rod is extracted out of the proximal end of the electrode lead to increase the flexibility of the lead. The electrode lead is then pushed forwards relative to the introduction shaft while the introduction shaft is retracted to maintain positioning of the electrodes around the DRG. Equal retraction of the introduction shaft and advancement of the electrode lead through the introduction shaft is critical to retain electrode placement around the DRG. Some excess electrode lead can be left in the spinal cord to prevent movement of the electrodes around the DRG after the implantation.

Procedure step 5: Retraction of the Tuohy needle. The needle is retracted from the epidural space through the same path of the insertion in between the spinous processes and out of the back. Careful retraction is critical to prevent electrode movement.

Result: Neurostimulation of the dorsal part of the DRG. The electrode lead is anchored to the outer soft tissue on the back and then connected to a neurostimulator. The result of the procedure is an implanted electrode lead array that surrounds the dorsal area of the dura around the DRG and the motor nerve.

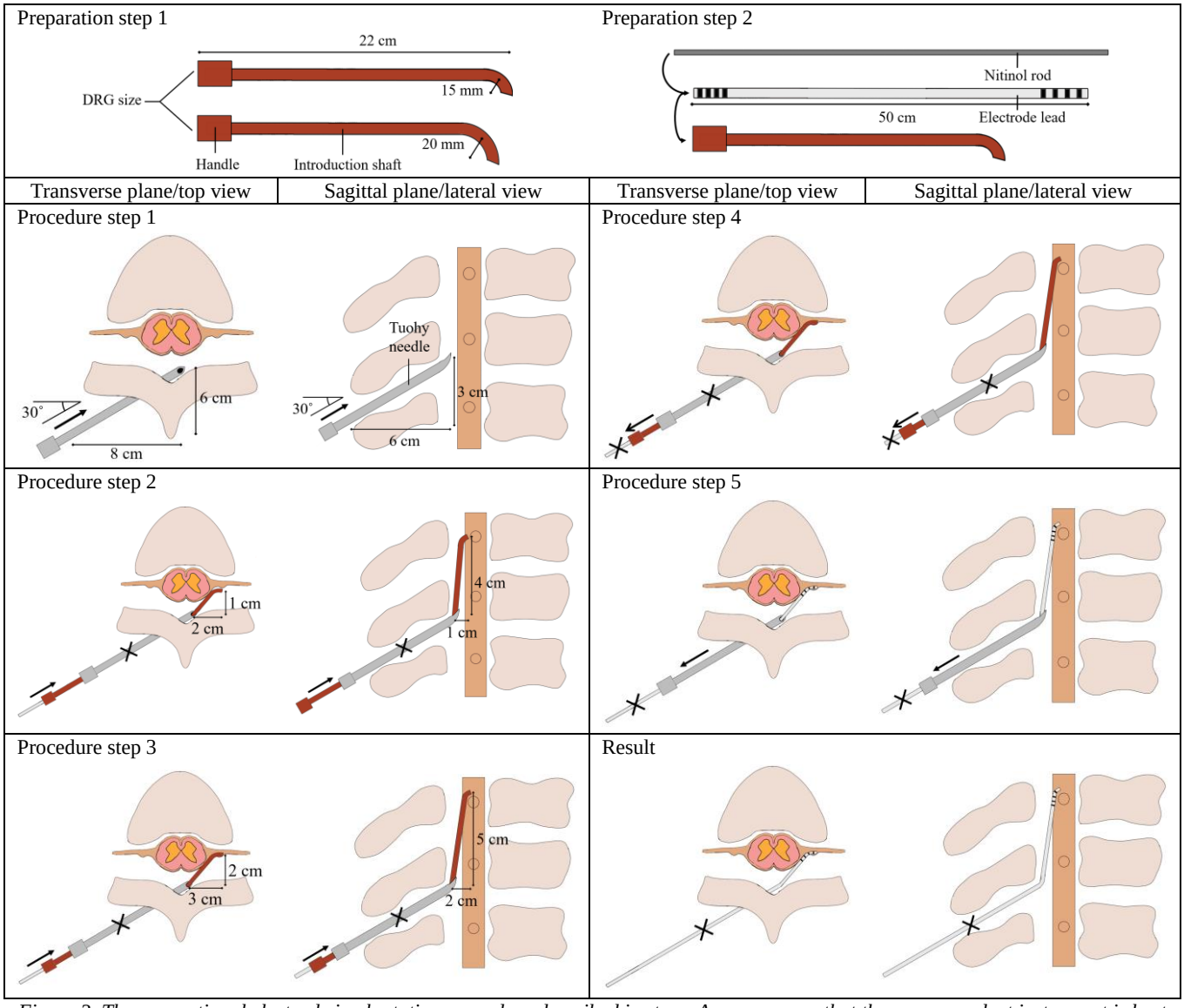

Figure 3. The conventional electrode implantation procedure described in steps. A cross means that the correspondent instrument is kept fixed during the step, an arrow means that the correspondent instrument is moved during that step in the direction of the arrow. The proximal squares on the needle and introduction shaft indicate handles. The drawings are not scaled, and the dimensions are rough estimates to indicate the travel distance of the instruments.

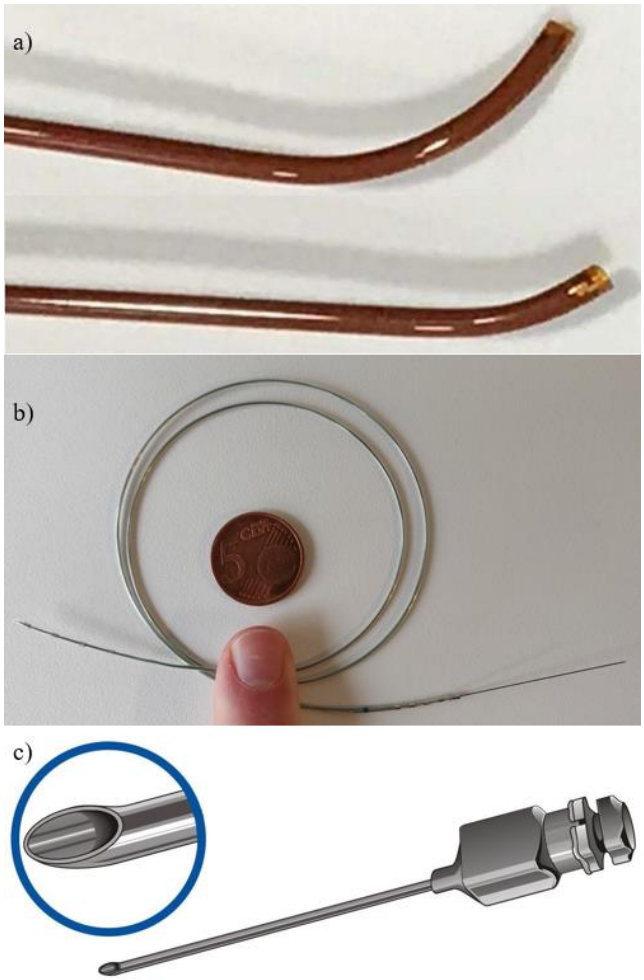

Figure 4. The conventional pre-curved electrode lead introduction shafts with a radius of curvature of 20 mm (top) and 15 mm (bottom) (adapted from [12]) (a). The electrode lead consists of a proximal (right) and distal (left) electrode array of four electrodes each and has an internal lumen to insert an included nitinol rod that sticks out on the proximal end (b). Tuohy needle with a close-up of the bevel-tip (adapted from [15]) (c). (Proximal and distal mean closest and furthest away to and from the body center and thus the physician using it in the implantation procedure respectively.)

1.3 State-of-the-art in steerable implantation instruments

A patent research was conducted on minimally-invasive steerable implantation instruments used to implant all types of "solid implants" such as neurostimulation electrodes, biopsy markers, vascular stent grafts, and heart valves. Common implantation instruments are composed of a handle, a tubular shaft, and an implant release mechanism. The maneuverability of the instrument shaft and the mechanism to release the implant affect the accuracy and precision to reach the target. A patent literature search was conducted using the Web of Science Derwent Innovations Index patent database. The mechanical designs, as described in the 122 relevant patents, were systematically classified in terms of shaft maneuverability and implant release mechanism. The shaft of the instrument was defined as rigid and straight, rigid and pre-curved, flexible and non-steerable, or flexible and steerable. The implant release mechanism was classified as reversible or irreversible, depending on the reusability of the connection between the instrument and the implant. Reversible release mechanisms were further classified as friction locks, shape locks, or magnetic locks. Irreversible release mechanisms were divided into a phase change or a chemical reaction of the connecting material between the implant and the instrument used to deploy the implant. No patents were found on mechanical disruption to irreversibly decouple an implant, thermal expansion to reversibly disengage a shape lock connection or multiple instrument techniques to improve instrument maneuverability or implant release.

1.4 Problem definition

According to Vancamp et al. [12], electrodes for DRG stimulation were incorrectly implanted in 12.8% (N = 78) of the patients in Spain before 2017. Several disadvantages of the conventional pre-curved introduction shafts used to implant the electrode leads can be a reason for the failed implantations:

- The introduction shaft tip has a fixed radius of curvature. When the DRG size is not correctly estimated before the start of the surgery, the radius of curvature of the introduction shaft tip must be changed to properly cover the DRG with the shaft tip. The only way to change the curvature on a pre-curved shaft is by replacing the shaft with another one with a different radius of curvature. However, the fixed curve on the introduction shaft tends to get damaged upon retraction through the Tuohy needle, as the pre-curved introduction shaft tip abrades along the sharp needle tip with the bevel angle. Subsequently, the fixed curve of the tip makes maneuverability along straight paths in the epidural space challenging, as the epidural fat creates an external lateral force on the curved tip in a perpendicular direction to the tip. This external force gives the shaft the tendency to move in a curved path instead of a straight path.
- The radius of curvature of the introduction shaft tips are too large to properly cover DRGs (Figure 5) and are only available with two different radii of curvature of about 15 mm and 20 mm. The introduction shaft tip should be as close to the DRG as possible for better neurostimulation. Optimally, electrode leads are implanted around the width of the DRG. The radius of lumbar and sacral DRGs is half of the width and is therefore 1 mm - 4 mm. Consequently, the minimum radius of curvature of the tip should be adjustable between 3.0 mm and 6.5 mm to properly cover all possible DRG sizes including a margin of 2 mm. The margin consists of extra space to prevent damage to the DRG (1 mm), the radius of the tip shaft (0.8 mm), and an extra margin for possibly larger DRG dimensions in other spinal regions (0.2 mm).
- The angle of curvature of the introduction shaft tips are too small and cover a maximum 25% of the DRG circumference. A larger electrode coverage of the DRG circumference, ideally 100%, would improve the stimulation, as DRG stimulation improves with a larger stimulation surface area. A larger coverage cannot be reached with multiple conventional introduction shafts, because the introduction shaft always reaches the DRG stimulation area at the dorsal DRG area in a clockwise direction from the dorsal area (Figure 5). Introduction shafts cannot reach the DRG in a counterclockwise direction because of the entry angle that the Tuohy needle should make to enter in between the spinous processes (Figure 1c) in the first procedure step.

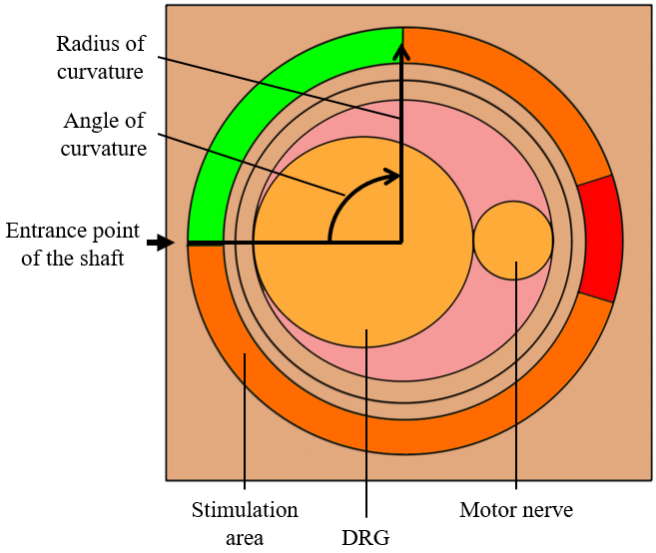

Figure 5. Stimulation area of the DRG and the motor nerve. The green and orange area indicate desirable DRG stimulation. The red area indicates undesirable motor nerve stimulation. The green area shows the maximum potential electrode coverage reached by implantation with conventional introduction shafts (25%). The radius of the dura is 1 mm to 4 mm. The minimum radius of curvature of conventional shafts is 15 mm. The entrance point of the shaft is on the dorsal area of the DRG.

1.5 Goal and layout of the thesis

The goal of this thesis is to design an electrode lead introduction shaft with a bendable tip in one direction to decrease the minimum radius of curvature of the implanted electrode leads around DRGs from 15 mm to an optimal 3.0 mm and increase the angle of curvature from 90˚ to an optimal 360˚ in order to improve neurostimulation against neuropathic pain.

The structure of this thesis is as follows. Design specifications are described in Section 2. Conceptual designs and proofs of principle of steering mechanisms are given in Section 3. In Section 4, the final design of the steerable introduction shaft is explained. Section 5 shows the manufacturing and assembly of the prototype. Experiments to validate the functioning of the prototype are described in Section 6, and the results of the experiments are given in Section 7. The design choices, results of the experiments, future recommendations, and remaining challenges are discussed in Section 8. Finally, the conclusions are given in Section 9.

2 Design requirements

2.1 Steerable electrode implantation procedure

This thesis describes the design of a steerable introduction shaft for electrode lead implantation. The implantation procedure using the steerable introduction shaft differs from the conventional implantation procedure (Figure 7). The steerable shaft should allow for manual adjustment of the minimum radius of curvature in the first preparation step instead of having to choose between pre-curved shafts with predetermined radii of curvature. The steerable shaft also allows for a combination of shaft translation and tip bending for a circular motion around the DRG in the third and fourth procedure step. The steerable shaft tip can be straightened for straight movement to the DRG in the second procedure step and bent to allow for curved forward and backward motion around the DRG in the third and fourth procedure step respectively. Instead of extracting the nitinol rod from the electrode lead in the fourth procedure step of the conventional procedure, the nitinol rod is extracted at the beginning of the third procedure step in the steerable implantation procedure to increase the flexibility of the steerable tip when bending around the DRG. The first and fifth procedure step remain similar as these steps do not involve the use of the introduction shaft. The result of the steerable implantation procedure is a circular electrode placement around the DRG instead of curved placement on only the dorsal DRG area in the conventional procedure.

2.2 Shaft requirements

The literature on conventional electrode implantation procedures for DRG stimulation and the anatomy of the spine, spinal cord and spinal nerves were analyzed to set up design requirements for the steerable electrode introduction shaft. The shaft is divided into three segments: a proximal end, distal end and steerable tip (Figure 6). The requirements are shown Table 1. A degree-of-freedom (DOF) is a desirable translation or rotation possibility that is not restricted by the design. A DOF is considered active if controlled internal forces cause elastic deformation. A DOF is considered passive if uncontrolled external forces cause desirable elastic deformation.

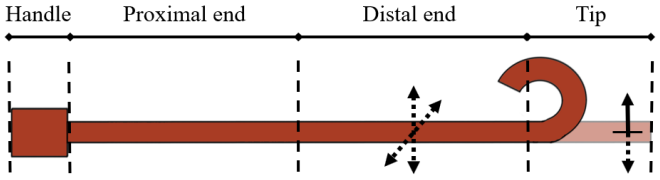

Figure 6. The steerable introduction shaft in a straight and bent configuration with the desired DOFs. The shaft is attached to a handle and has a proximal end, distal end, and steerable tip. The solid arrow shows the active DOF in one direction of the tip. Dotted arrows show passive DOFs.

Part → Requirement ↓	**Proximal end**	**Distal end**	**Tip**
Inner diameter [mm]	> 1.1	> 1.1	> 1.1
Outer diameter [mm]	< 1.6	< 1.6	< 1.6
Length [mm]	< 150	> 70	20
Minimum radius of curvature [mm]	-	-	< 15.0 (optimal 3.0)
Maximum angle of curvature [˚]	-	-	> 90˚ (optimal 360˚)
Active DOF	-	-	1 (in one direction)
Passive DOF	-	2	2 (from which one in one direction)
Stiffness	No buckling during insertion into needle.	Bending through bevel-tip of needle.	Sideways motion through epidural fat.

Table 1. Design requirements of the introduction shaft.

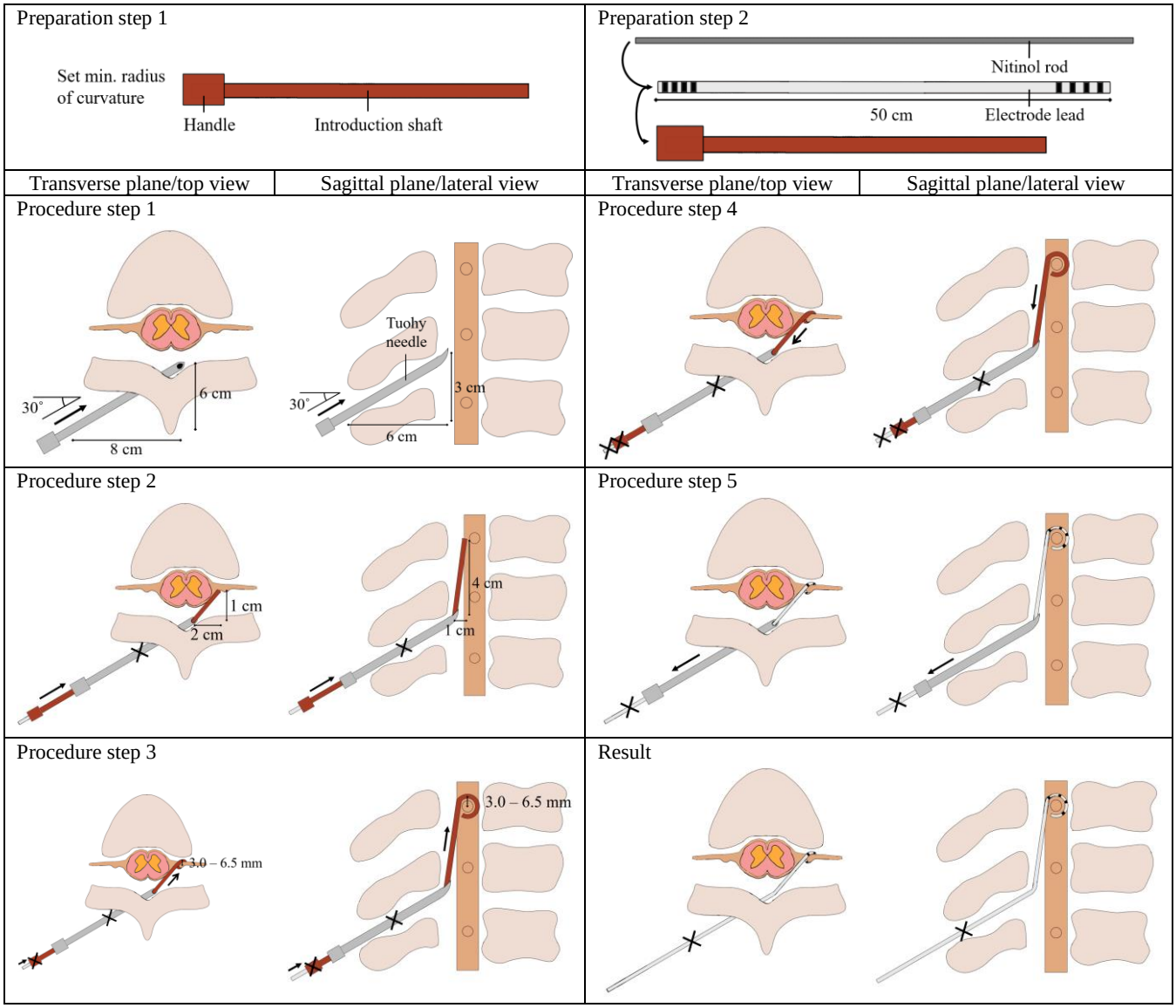

Figure 7. The steerable electrode implantation procedure described in steps. A cross means that the correspondent instrument is kept fixed during the step, an arrow means that the correspondent instrument is moved during that step. The proximal squares on the needle and introduction shaft indicate handles. The drawings are not scaled. The dimensions, except for the tip radius of curvature, are rough estimates to indicate the travel distance of the instruments.

2.2.1 Proximal end

- *The minimum inner diameter is 1.1 mm.* The inner diameter of the shaft is limited by the outer diameter of the electrode lead (1.0 mm). A 0.1 mm margin is added to prevent the electrode lead to stick in the shaft upon retraction.
- *The maximum outer diameter is 1.6 mm.* The outer diameter of the shaft is limited by the inner diameter of the Tuohy needle (1.7 mm). A 0.1 mm margin is added to prevent the shaft to stick inside the needle.
- *The minimum length is 150 mm.* The proximal end length is the sum of the Tuohy needle length without the bevel-tip (100 mm) and a 50 mm margin to attach the shaft to the handle.
- *The proximal end should not buckle during insertion.* The proximal end should be stiff enough to withstand external forces of the needle that act on the shaft during shaft insertion through the needle in the second procedure step.

2.2.2 Distal end

- *The minimum inner diameter and maximum outer diameter are equal to those of the proximal end.*
- *The minimum length is 70 mm.* The distal end length is the sum of the Tuohy needle bevel-tip length (10 mm) and the distance from the Tuohy needle tip to the DRG in the second procedure step (80 mm), minus the length of the steerable needle tip (20 mm, Section 2.2.3).
- *The distal end should move through the bevel-tip of the needle end and have two passive DOFs.* The introduction shaft bends through the bevel-tip of the Tuohy needle in the second procedure step and should not plastically deform the needle tip or the distal end of the shaft. The distal end should be flexible enough to bend with two passive DOFs in all the directions towards the inner Tuohy needle shaft.

2.2.3 Tip

- *The minimum inner and maximum outer diameter are equal to those of the proximal and distal end.*
- *The length is 20 mm.* The currently used electrode array has a total length of 20 mm and should be covered completely by the tip. Large DRGs cannot be covered by the electrode array completely, as a large DRG requires a tip radius of curvature of 6.5 mm (Section 1.4) and a

circumference of 41 mm. For large DRGs, the choice was made to cover only the top half of the desirable DRG surface and not the whole circumference to stimulate the bottom half of the desirable DRG surface (Figure 8), as a variable bendable tip length complicates the shaft and handle design significantly. Currently, the results of top half and bottom half DRG stimulation are comparable. However, a longer tip that can surround large DRGs completely becomes a better option when longer electrode arrays with more and smaller electrodes will become available, as discussed in Section 8.4.

- *The minimum radius of curvature is smaller than 15.0 mm (optimally 3.0 mm).* The tip should achieve a smaller minimum radius of curvature than conventional introduction shafts (15.0 mm). Optimally, the minimum radius of curvature of the tip should be adjustable between 3.0 mm and 6.5 mm to properly cover all possible DRG sizes (Section 1.4). The design specification of the tip only states the minimum radius of curvature, as the adjustability to a larger minimum radius of curvature for relatively larger DRGs is provided by the handle.
- *The maximum angle of curvature is larger than 90˚ (optimally 360˚).* The tip should achieve a larger maximum angle of curvature than conventional introduction shafts (90˚) to increase the DRG circumference coverage by the implanted electrode lead. Optimally, electrode leads are implanted around the whole DRG circumference (360˚). The angle of curvature can be calculated with the radius of curvature and the length of the tip if the tip bends with a circular shape. The angle of curvature requirement helps to verify proper tip functioning if the tip does not bend with a perfect circular shape.
- *The tip has a single active DOF in one direction.* A single active DOF in one direction allows for bending around the DRG and straightening for straight movement inside the epidural space and the Tuohy needle to diminish shaft abrasion along the bevel-tip of the needle.
- *The tip should move sideways through epidural fat.* The epidural fat limits the flexibility of the tip. The tip should not buckle when it is pushed through the epidural space towards the DRG. Sideways motion through the fat is required in certain situations and sideways motion is the worst-case scenario in terms of stresses on the tip. Therefore, the tip should have two passive DOFs in the perpendicular directions to the shaft. These passive DOFs give the tip shaft flexibility to bend passively with elastic deformation by external forces in the lateral directions of the tip shaft. One of these DOFs is however only passive in one direction, as the DOF in the other direction is the abovementioned active DOF in one direction. The assumption was made that the mechanical properties of epidural fat are similar to other body fats. Proper functioning of the tip through fat is to be verified experimentally.

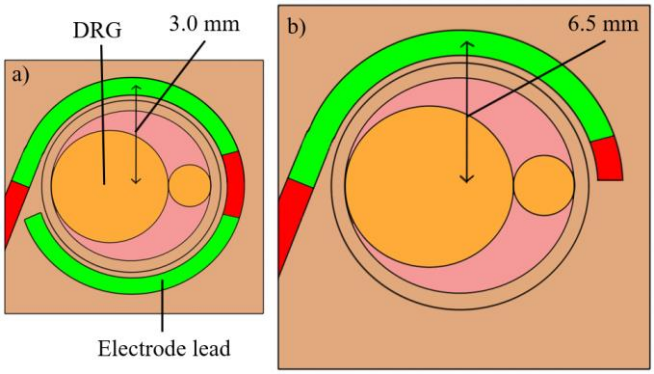

Figure 8. Electrode placement around relatively small (a) and large (b) DRGs with desirable (green) and undesirable (red) neurostimulation of the electrodes.

2.3 Handle requirements

The proximal end of the shaft is connected to a handle to improve control during the procedure. The handle has requirements for the control mechanism and for ergonomics.

2.3.1 Control mechanism

- *The handle has a control mechanism to adjust the minimum radius of curvature of the steerable tip between 3.0 mm and 6.5 mm.* The handle can adjust the minimum radius of curvature of the tip between 3.0 mm to 6.5 mm (Section 2.2.3) in the first preparation step to properly cover all possible DRG sizes.
- *The handle provides combined tip bending and shaft translation relative to the handle for circular tip motion.* A mechanical solution in the handle allows for pre-defined control of a circular tip motion around the DRG by providing simultaneous tip bending and shaft translation relative to the handle in the third procedure step.
- *The handle allows for shaft rotation.* With a handle, torque can be applied with the wrist instead of with the fingers on a shaft without a handle. Torque application on the shaft is critical to rotate the shaft inside the Tuohy needle in the second procedure step.
- *The handle has a mechanism to lock the minimum radius of curvature adjustment control and the circular tip motion control independently.* The minimum radius of curvature adjustment is only adjusted in the first preparation step. The circular tip motion is only required in the third and fourth preparation step. Locking of the control mechanisms is required to prevent unintentional use during other implantation steps.

2.3.2 Ergonomics

- *The handle can be used with a single hand.* The handle should be controlled with one hand as the other hand is used to hold the Tuohy needle and to keep the electrode lead fixed around the DRG upon shaft retraction.
- *Handle control is done with the thumb and index finger for precision.* The thumb and index finger have more control precision compared to other fingers [17] and should, therefore, be used to control the minimum radius of curvature adjustment and the circular tip motion.
- *The handle has a proximal hole to insert the electrode lead.* The handle has a proximal hole for electrode insertion and retraction in the introduction shaft.
- *The handle has a distal hole to insert the introduction shaft and to prevent shaft rotation relative to the handle.*

The handle has a distal hole to attach the introduction shaft. The distal hole should prevent rotation of the shaft relative to the handle, as the handle is used to rotate the tip.

3 Steering mechanism

3.1 Conceptual design

Steerable shafts can be actuated with different types of force generation [18, 19]. The following classification structure (Figure 9) shows actuation types for steerable shafts through soft tissue with a single DOF in one direction. First, a division is made between instruments with internal and external actuation. With internal actuation, force is generated inside the shaft and energy is delivered to the actuator. With external actuation, force is generated outside the shaft and transmitted to the tip. Internal actuation is further classified as electric, thermal, or magnetic actuation. External actuation is further classified as hydraulic chamber or mechanical actuation.

Internal actuation impractical because of the small dimensions in the design requirements. Electric force generation is not feasible because of bending limitations and questionable safety, thermal force generation because of overheating and complicated manufacturing, and magnetic force generation because of insufficient force generation to steer through soft tissue. With external actuation, hydraulic chamber actuation is not feasible because of discontinuous bending control and safety requirements. Mechanical actuation was chosen to be the most feasible solution because of simple force generation of the human muscles of the physician and no need for energy supplies.

Mechanical actuation solutions are further classified to instruments with or without internal pulling cables (Figure 10). Most mechanically actuated steerable shafts make use of an internal cable that is attached to the tip. Pulling the cable results in a bending motion of the shaft. The internal cable can be attached to single segments, to serial segments, or to one of the shafts in concentric shaft designs. A tip with pre-bent concentric shafts is the only found solution type without a pulling cable.

Further distinction was made between active and passive bending and between continuous and discrete bending. Active bending provides controlled manipulation of the radius of curvature of the shaft, while passive bending is done with an uncontrollable radius of curvature. A continuous bend has a smooth circular shape, while a discontinuous bend has repetitive straight parts in the curve due to differences in material stiffness. All mechanical solutions with a pulling cable for steering have active bending, as pulling force on the cable manipulates the radius of curvature.

Single segmented shafts are comprised of one part and can use strain on the material of the whole shaft to make a curve (Figure 11a). Symmetric shaft shapes allow for continuous bending, as the whole shaft is strained equally when a pulling force is exerted on the shaft. Holes, slots, or other manipulations to the shaft allow for discontinuous and more flexible bending of the shaft, as the pulling force is not distributed equally over the shaft.

Serial segmented shafts have several unbendable connected parts. The shafts can bend discontinuously by moving the parts relative to each other (Figure 11b). Segmented shafts are flexible and can prevent bending in undesirable directions with the shape of the segments. However, segmented shafts need a rod on the opposite side of the cable to flex the shaft back to a straight position when tension on the cable is released.

Concentric shafts consist of two overlapping shafts with an attached cable to one of the shafts (Figure 11c). Pulling of the attached cable causes relative translation of the shafts to bend the assembly, as each shaft has a different stiffness. Concentric shafts have precise passive bending with the translation of the shafts but are not feasible for the diameter constrictions of the design requirements. Concentric shafts only bend passively as the curvature depends on the fixed stiffness of the shaft material.

Pre-bent concentric shafts consist of multiple pre-curved overlapping shafts (Figure 11d). Pre-bent concentric shafts lack an attached cable, as the translation of the shafts relative to each other causes passive bending of the assembly due to different stiffnesses of the shafts. However, the pre-curved shafts have a predetermined curve that prevents active bending of the assembly.

The single segmented shaft was chosen as the best steering mechanism, because of active bending functionality, flexibility between continuous and discontinuous bending and compliance. An internal cable runs through the shaft and is attached to the distal end to allow for equal force distribution over the shaft material when pulling the cable. Lateral gaps provide a naturally preferred bending direction in the direction of the cable.

The steering mechanism in the steerable electrode lead introduction shaft should only bend the tip. A single segmented nitinol tip design with lateral slots (Figure 11a) was chosen to facilitate bending on the side of the cable and prevent bending in the opposite direction. The increased flexibility does entail discontinuity of the curve, but many thin instead of few large slots can diminish this problem. The dimensions of the slots were calculated with an article from York et al. [20] that describes the design of a single segment steerable nitinol shaft. The minimum and maximum radius of curvature, tip length, and inner and outer diameter from the design requirements were used as constants to find the dimensions of the slots. A pre-defined number of seven lateral slots was chosen, along with a 0.90 mm depth of the cuts. Consequently, the specified minimum radius of curvature was calculated to be reached with a slot width of 0.88 mm with 1.97 mm in between the cuts (Figure 12). With these dimensions, the tip was calculated to reach a maximum angle of curvature of 301˚. A similar design was made with a slit in the shaft wall through which the pulling cable was guided through, with the advantage that the cable does not create friction on the electrode lead. The design consisted of two concentric shafts where a slit was drilled on the outside of the inner shaft. The lateral slots could be drilled from the side once the two shafts were assembled together.

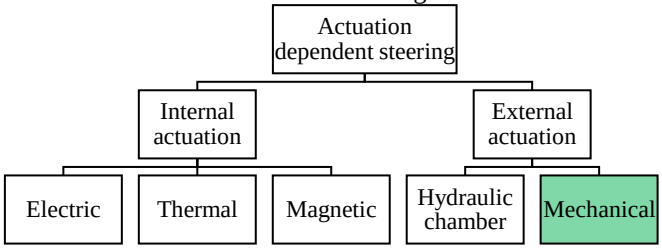

Figure 9. Classification structure of actuation types for steerable shafts through soft tissue with a single DOF in one direction. The green block shows the selected type of actuation for the final design.

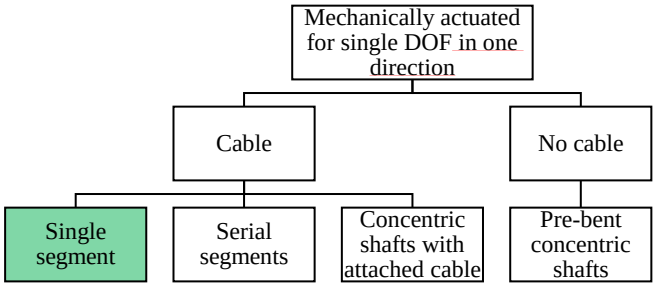

Figure 10. Classification structure of mechanical actuation types for steerable shafts through soft tissue with a single DOF in one direction. The green block shows the selected type of actuation for the final design.

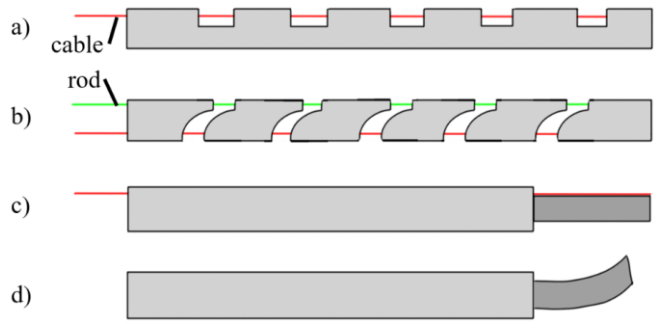

Figure 11. Mechanical tip actuation solutions with a single segment (a), serial segments (b), concentric shafts with an attached cable (c), and pre-bent concentric shafts (d).

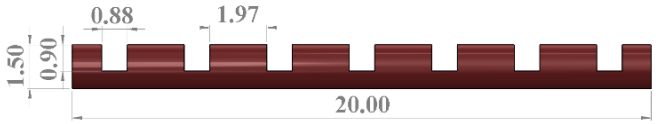

Figure 12. The single segmented nitinol tip design with lateral slots with dimensions in mm. The pulling cable is not shown.

3.2 Concept prototyping

Several proof of principles of the steerable tip were created. All the shaft tip prototype iterations are explained in chronological order. The final tip design is described in Section 4.1.

First, a stainless-steel shaft with a 1.6 mm outer diameter and a 1.1 mm inner diameter was used to see if similar flexibility could be reached as with the nitinol shaft described by York et al. [20]. Slots on the side of the tube were filed of the tube with a circular miniature file (Figure 13a). A file was used instead of a drill to minimize manufacturing costs and to prevent plastic deformation caused by heating of the drill. A cable was guided through the inner lumen and attached to the distal end of the tip with a knot. The stainless-steel shaft design was infeasible, as cable pulling only caused a tip displacement of about 1 mm, and extensive pulling caused plastic deformation of the steel in the proximal slot before reaching the specified minimum radius of curvature. Nitinol shafts were considered as nitinol provides more flexibility than stainless-steel, but nitinol shafts were not used because of pricing.

Second, a polyester shrinking tube (VENTON Medical Group) was used with a 2.2 mm inner diameter before shrinking. The shrinking tube was heated up slightly around a catheter with a similar outer diameter as the electrode lead (1.0 mm) to acquire the correct outer and inner diameter and to increase the flexibility of the tube. The catheter was removed (Figure 13b) or kept inside the shrinking tube (Figure 13c). No lateral cuts were made in the shrinking tube as the shrinking tube was too fragile. The pulling cable was glued with Pattex Gold glue [21] to one side of the shrinking tube in between two slots that were cut with a Swann-Norton number eleven scalpel blade [22]. A stainless-steel rod was glued to the other side of the shrinking tube to straighten the shaft after bending. The shrinking tube design was infeasible as the glue that attaches the rod to the shrinking tube let go after a few hours. The shrinking tube also buckled before reaching the specified minimum radius of curvature.

Third, another slotted design was made from standard neoprene electrical wire with an outer diameter of 2.5 mm. A 25 mm long piece was cut, and the outer plastic shaft was stripped from the copper. The shaft was stretched around a needle with a 1.3 mm outer diameter (Figure 13d). The lateral slots and the distal cable groove were cut in the shaft with a Stanley-knife, and the pulling cable was glued [21] to the distal outer groove. A more precise model was created by making the cuts with a surgical scalpel [22] under a microscope with 50 times zoom (Figure 13e). The plastic shaft could reach the 3.0 mm radius of curvature and the plastic had good adhesion with the pulling cable and the glue. However, the elasticity of the shaft was low as the shaft did not straighten completely after bending without applying external forces. The outer diameter was 2.3 mm and was therefore larger than the specified maximum outer diameter.

Fourth, a 3D-printed tip was created with R5 ABS liquid photopolymer. R5 is a flexible material with a tensile strength of 31-39 MPa and a flexural modulus of 1190-1383 MPa [23]. The models were printed with a high precision (15-100 µm) with the EnvisionTec Perfactory 4 Standard SLA 3D-printer. The single segmented tip design described in Section 3.1 was printed with four different lateral slot depths of 0.9, 1.0, 1.1 and 1.2 mm (Figure 13f). All the models reached the required radius of curvature, but the material was too fragile and brittle as the tips broke after bending them multiple times.

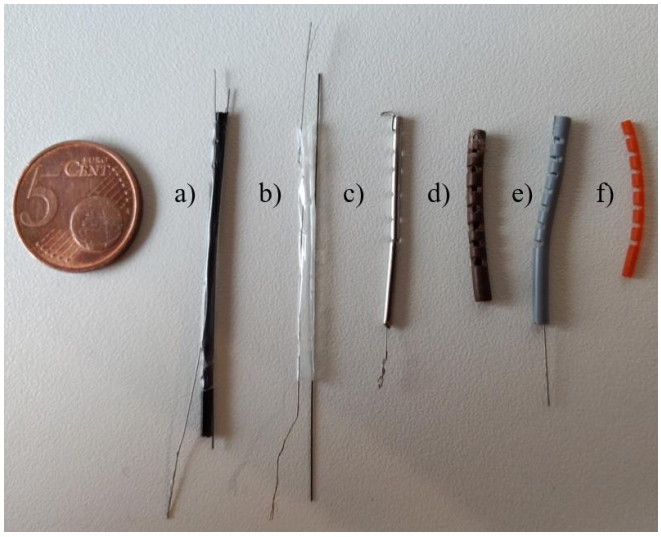

Figure 13. Iterations of the steerable tip prototypes that were not chosen as the final prototype, consisting of a filed stainless-steel capillary tube (a), a nitinol rod glued to a shrinking tube without (b) and with (c) an internal catheter, a cut and stripped electricity wire with lateral cuts done without (d) and with (e) a microscope, and an R5 ABS 3D-printed tip (f).

4 Final design

4.1 Shaft design

The design of the shaft is divided in the design of the proximal end, distal end and the shaft tip (Figure 14a).

Proximal end. The proximal end of the introduction shaft only moves inside the Tuohy needle and no bending is required, because the proximal end only moves inside the Tuohy needle. Therefore, it can be infinitely stiff. The proximal end has a length of 150 mm and is long enough to reach the beginning of the bevel-tip of the Tuohy needle and have a margin to be attached to the handle. The inner diameter is 1.1 mm and the outer diameter is 1.6 mm. One side of the proximal end has half of the circumference cut out to provide a shape lock in the handle to prevent rotation of the shaft inside the handle (Figure 14b).

Distal end. All the design requirements of the distal end are already met by the conventional pre-curved shafts. Therefore, a part can be cut from the straight part of the conventional pre-curved shafts to serve as the distal end of the steerable introduction shaft. The length of the distal end is 70 mm, the inner diameter is 1.1 mm and the outer diameter is 1.6 mm (Figure 14c).

Tip. For the steerable tip, a new design was created with a nitinol rod that is clamped in between pieces of stainless-steel capillary tube (Figure 15). The two pieces of capillary tube that are clamped over each other are called rings and the rod cannot slide through the rings as the deformation of the rings creates a clamping force on the nitinol rod. This design is cheaper to manufacture than the nitinol rod design from York et al. [20] as stainless-steel capillary tubes and nitinol rods are cheaper than nitinol capillary tubes with similar dimensions. The friction of the stainless-steel rings on the nitinol rod is crucial to prevent translation of the rings over the rod. Rings with a width of 2.0 mm were verified to provide enough friction to prevent movement of the nitinol rod in between the rings. A nitinol rod with a diameter of 0.25 mm was verified to provide enough flexibility and elasticity for the specified minimum radius of curvature. Optimization of the smallest possible ring width to provide enough friction on the nitinol rod and optimization of the rod diameter was not within the scope of this thesis. Consequently, as the stainless-steel rings are slightly wider and have a higher stiffness than the nitinol design of York et al. [20], the design has six rings instead of eight with a total tip length of 22 mm, as six rings is the maximum number of rings to reach the minimum radius of curvature of 3.0 mm. Subsequently, because of the stiffer stainless-steel rings, the tip is 2.0 mm longer than the electrode array length of 20 mm, as the proximal part of the tip is a ring that bends negligibly. The pulling cable can be made from nitinol or braided stainless-steel wiring. Nitinol is more flexible and elastic, but stainless-steel can be glued and is cheaper. A 0.15 mm diameter braided stainless-steel cable was verified to be strong enough to withstand pulling forces that could easily bend nitinol rods with a 0.25 mm diameter sufficiently. The cable was also thin enough to fit in between the electrode lead and the introduction shaft and was flexible enough to reach the curve in the steerable shaft tip. The pulling cable runs through the shaft and is attached to the most distal ring.

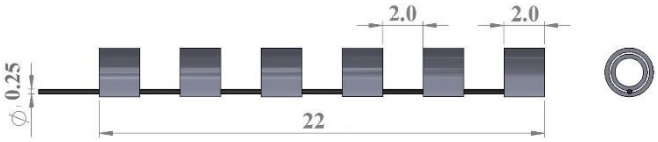

Figure 15. The final steerable tip design with clamped stainless-steel rings on a nitinol rod with dimensions in mm. The pulling cable is not shown.

4.2 Handle design

The handle consists of a bending trigger, radius adjustment button, bending trigger lock, radius adjustment button lock, shaft rack, front and rear casing parts, two lock catches, custom machined screws, and standard M5 nuts (Figure 16) (Appendix A). All the designed parts are explained separately, along with the method of use of the handle for every steerable implantation step.

4.2.1 Bending trigger

The bending motion of the steerable tip should be the most precise and critical motion control of the handle. Therefore, the index finger was chosen to control the bending of the tip, and a trigger on the handle is a solution for index finger motion (Figure 17). The bending trigger has a finger-hole to facilitate motion in two directions and achieve bending and straightening of the steerable tip. The hole has a diameter of 22 mm to provide a comfortable index finger fit.

The bending motion of the tip should be combined with translational motion of the shaft to achieve a circular motion of the tip around the DRG in the third and fourth procedure step. Translational motion of the shaft can achieve bending of the tip if the cable of the tip is fixed inside the handle. A rack-and-pinion system is used to convert the rotational motion of the trigger into translational motion of the shaft. The shaft is connected to a rack, and the rack is in contact with a proximal gear on the trigger. Dimensions of the gears are defined by the maximum translational motion that the trigger should achieve to fully bend the steerable tip. The maximum translational motion is the length of the cable that should be pulled to fully bend the tip and can be calculated by subtracting the

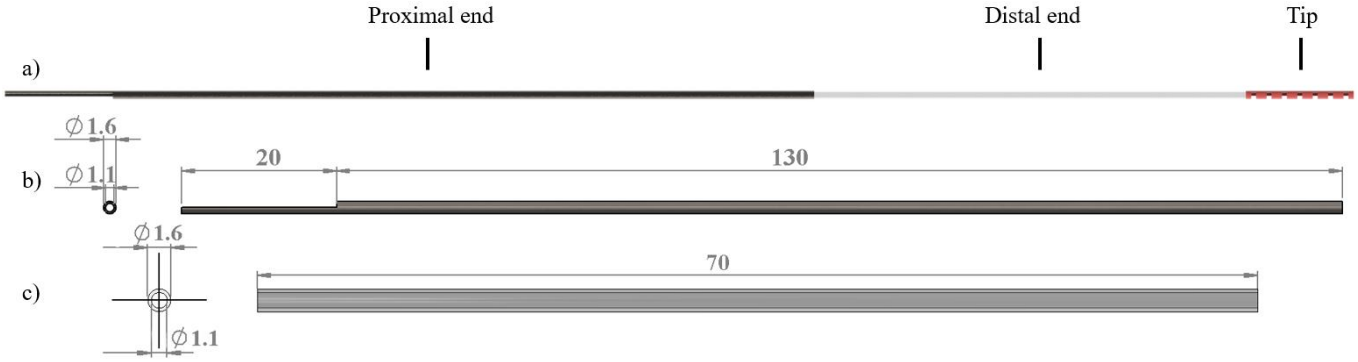

Figure 14. The shaft assembly (a). The proximal end with dimensions in mm. The left side has half of the circumference cut out (b). The distal end with dimensions in mm (c).

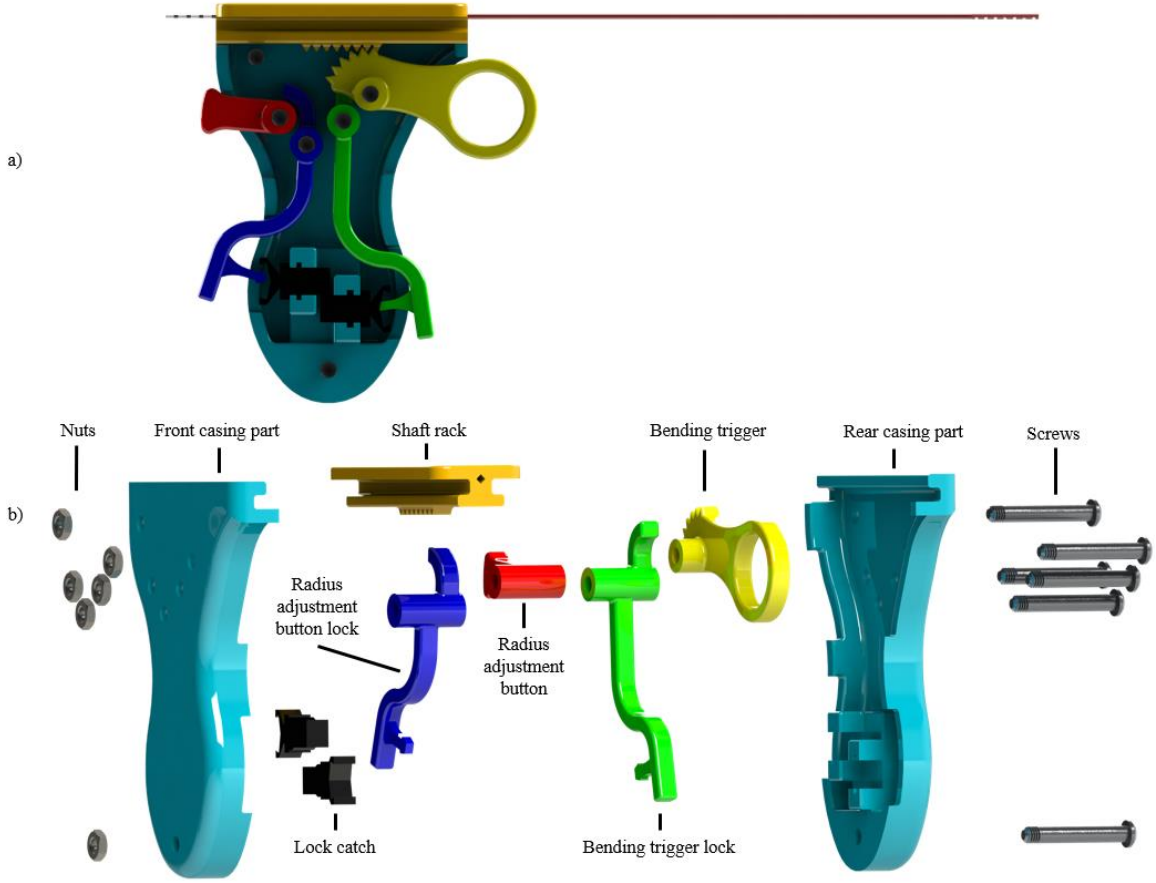

Figure 16. The assembled handle without the front casing part (a), and an exploded view of all the handle parts (b).

minimum radius of curvature difference between the cable and the tip multiplied with the maximum angle of curvature from the total tip length. The diameter of the gear on the trigger can then be calculated by multiplying the pulled cable length with a chosen maximum trigger rotation of 45˚. Consequently, the trigger gear radius is 12.0 mm including a 3.2 mm margin to make up for cable stretching and bending of the proximal and distal end of the shaft. All the calculations were done in the Python programming language in Microsoft Visual Studio Code (Appendix B).

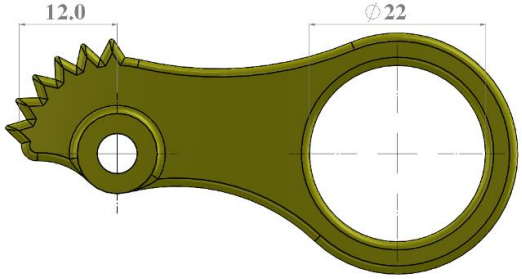

Figure 17. The bending trigger with dimensions of the index-finger-hole and the gear radius in mm.

4.2.2 Shaft rack

The steerable shaft is connected to a shaft rack to convert the rotational motion of the bending trigger to translational motion of the shaft. The shaft is connected to the shaft rack with a rectangular part that has a distal hole to pass through the shaft, and a proximal hole to pass through the electrode lead (Figure 18a). The holes are squared to simplify manufacturing if the shaft rack is 3D-printed. The distal hole for the shaft rack has a half square extrusion in the proximal 20 mm of the hole to provide a shape lock with the proximal shaft end and prevent rotation of the shaft inside the shaft rack. The rack length is defined by the maximum pulled cable length to fully bend the steerable tip and is 21 mm including a 14 mm margin to make up for stretching of the cable and bending of the proximal and distal end of the shaft, as well as extra length to place the trigger gear on the rack. The margin is also kept relatively large as there is enough space for translation inside the casing anyway. A slit is made on the proximal side for the cable to run down from the introduction shaft to the radius adjustment button (Figure 18b). The slit has a circular shape to prevent sharp curves in the cable to decrease friction.

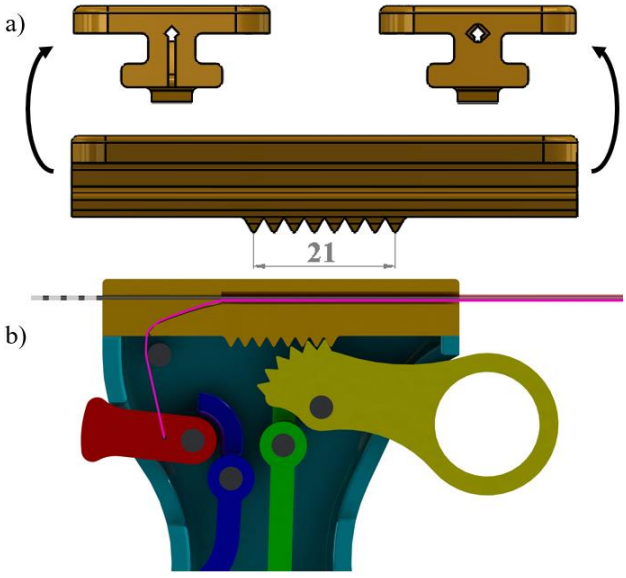

Figure 18. The shaft rack (a) with the rack length in mm and views of the electrode lead hole (left) and the introduction shaft hole (right), and a drawing of the cross-section of the handle with the cable in pink that runs through the rack part and attaches to the radius adjustment button (b).

4.2.3 Radius adjustment button

The pulling cable inside the introduction shaft runs down through the shaft rack inside the handle. Instead of attaching the cable to the handle, the cable is attached to the radius adjustment button. The cable is inserted through the hole on the button (Figure 19) and can be attached with a knot around the circular axis. The button rotates around the axis and the end of the button has a large rectangular surface, as the button is to be controlled with the thumb. The radius adjustment button serves as an extra tool to adjust the minimum radius of curvature of the steerable tip in the first preparation step without bending the tip. The attached cable is fully tightened when the button is in the downward position to allow for a small radius of curvature of the tip when the bending trigger is moved downwards to surround relatively small DRGs. In the upward position, the pulling cable is not fully tightened to allow for a larger radius of curvature of the tip when the bending trigger is moved downwards to surround relatively large DRGs.

The distance from the rotating axis to the cable hole defines the amount of cable travel that the button can generate. The cable travel is defined by the cable length difference between fully bending the tip from the lowest to the highest minimum radius of curvature setting. The diameter can be calculated by dividing the cable travel by the chosen maximum button rotation of 45˚ multiplied by the sinus of the maximum button rotation. Consequently, the distance from the cable hole to the axis of the button is 6.0 mm including an estimated 1.5 mm margin to make up for cable stretching and bending of the proximal and distal end of the shaft. All the calculations were done in the Python programming language in Microsoft Visual Studio Code (Appendix B).

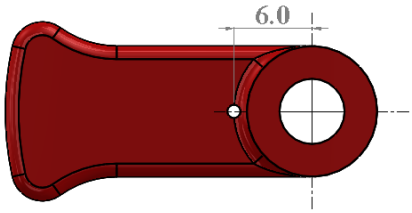

Figure 19. The radius adjustment button with the distance between the rotation axis and the pulling cable hole in mm.

4.2.4 Bending trigger and radius adjustment button locks

The handle consists of two individual locking mechanisms to lock the radius adjustment button and the bending trigger to restrict movement of the button and the trigger when they are not utilized in certain steps of the procedure (Figure 20a-b). The locks rotate around an axis and have a curved top that fits exactly around the axis of the button and the trigger. Friction is created between the curved top and the button axis when a force is applied in the direction of the pins at the bottom of the locks. The pins at the bottom of the locks fit exactly in lock catches in the handle and can be locked with a single push and unlocked with another push in the direction of the pin (Figure 20c) [24]. The lock catches in the handle are locking mechanisms from Brabantia trash cans (Brabantia Branding B.V., Valkenswaard, The Netherlands) to open and close the cans.

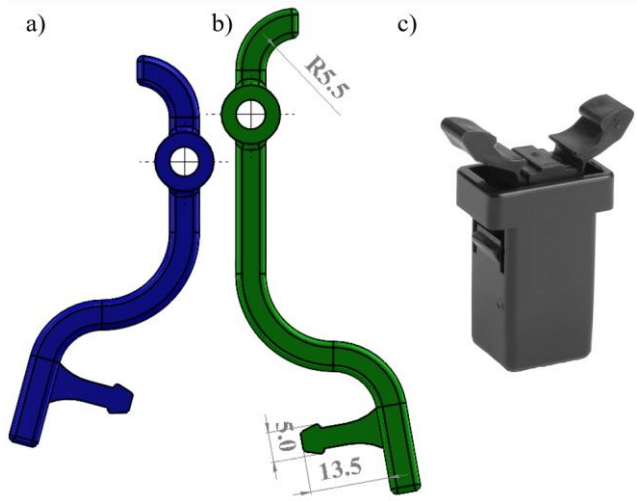

Figure 20. The radius adjustment button lock (a), the bending trigger lock (b), and the lock catch (c) [24], with dimensions of the friction curve and the lock pin in mm.

4.2.5 Casing

The casing of the handle holds other handle components and the introduction shaft in place (Figure 21). The casing is kept as small as possible with smooth edges and curved notches to provide a comfortable grip. The casing, including the rack part, has a length, width and depth of 120, 75 and 29 mm respectively. The casing consists of a front and rear casing part to simplify assembly of the internal parts. The rear casing part is a mirrored version of the front casing part, except for an extruded rectangular center part to hold the lock catches in place. The two casing parts are kept together with custom made screws that function as rolling axes for the internal parts and the cable. A nut is attached to the threaded distal end of the screw axis to hold the casing together along with all the internal parts. The top of the casing has lateral slits to allow translational sliding of the shaft rack. Notches in the middle allow movement of the extruding bending trigger, radius adjustment button and locks in a desirable range.

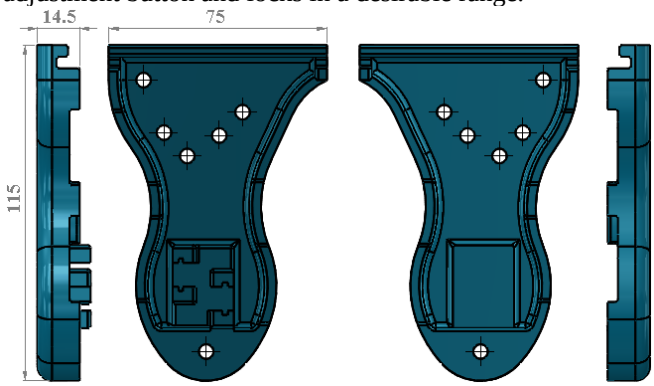

Figure 21. The rear (left) and front (right) part of the casing with dimensions in mm.

The casing of the handle is kept together with custom screws (Figure 22) and standard M5 nuts. The screws have a total length of 35.0 mm and includes a non-threaded 29.0 mm equal to the width of the casing, a distal threaded 4.0 mm equal to the width of a standard M5 nut, and a proximal 2.0 mm with a larger diameter to prevent translation of the tip in the casing. The tip has a diameter of 8.0 mm and the rest of the screw has a diameter of 4.9 mm for the M5 thread on the distal end and a 0.1 mm margin to prevent sticking of the screws in the 5.0 mm holes of the casing. The tip has no slit for a screwdriver as not much force is required to tighten the screws in the nuts.

Figure 22. The machined screws with dimensions in mm.

4.2.6 Method of use

The method of use of the handle is explained for every step in the implantation procedure that involves use of the handle (Figure 23). The steps that involve the use of the handle are the first and second preparation steps and the second, third and fourth procedure steps. The first and fifth procedure step do not involve use of the handle and are not described in this Section.

Preparation step 1: The radius adjustment button is used to adjust the minimum radius of curvature of the steerable tip. For large DRGs, the button is put in the upward position. For small DRGs, the button is put in the downward position. The button can be set in any position between the upward and downward position. After selecting the minimum radius of curvature, the radius adjustment button lock is pushed to lock the radius adjustment button for the rest of the implantation procedure.

Preparation step 2: The electrode lead is inserted in the proximal hole of the shaft rack. Rotation of the lead during translation prevents the lead from sticking inside the shaft. Further use of the handle is not required.

Procedure step 1: The handle is not used during the needle insertion.

Procedure step 2: The introduction shaft is inserted in the proximal end of the Tuohy needle by moving the handle towards the needle. Translation and rotation of the handle ensure a proper angle of the introduction shaft in the epidural space until the tip is positioned as close to the dorsal side of the DRG as possible.

Procedure step 3: The bending trigger is moved downwards to translate and bend the introduction shaft tip around the DRG. The trigger is moved downwards until the trigger cannot move any further. Before using the bending trigger, the nitinol rod inside the electrode lead is extracted to increase flexibility of the steerable tip. Once the tip is positioned around the DRG, the radius adjustment button can be unlocked and moved upwards or downwards slightly to adjust the minimum radius of curvature if the DRG size is smaller or larger than expected. Adjustment of the minimum radius of curvature after bending is only optional to prevent DRG damage. The radius adjustment button is locked again after using the radius adjustment button.

Procedure step 4: *The bending trigger is moved upwards while the electrode lead is kept at the same position relative to the casing. The handle is then retracted while the electrode lead is pushed forwards through the proximal end of the shaft rack with an equal distance.* Consequently, the introduction shaft tip is retracted in the same circular path as in the third procedure step and in the same translational path as in the second procedure step, while the electrode array remains fixed around the DRG. Once the bending trigger is again in the upward position, the bending trigger lock can be used optionally to lock the bending trigger.

Procedure step 5: The handle is not used during the needle extraction.

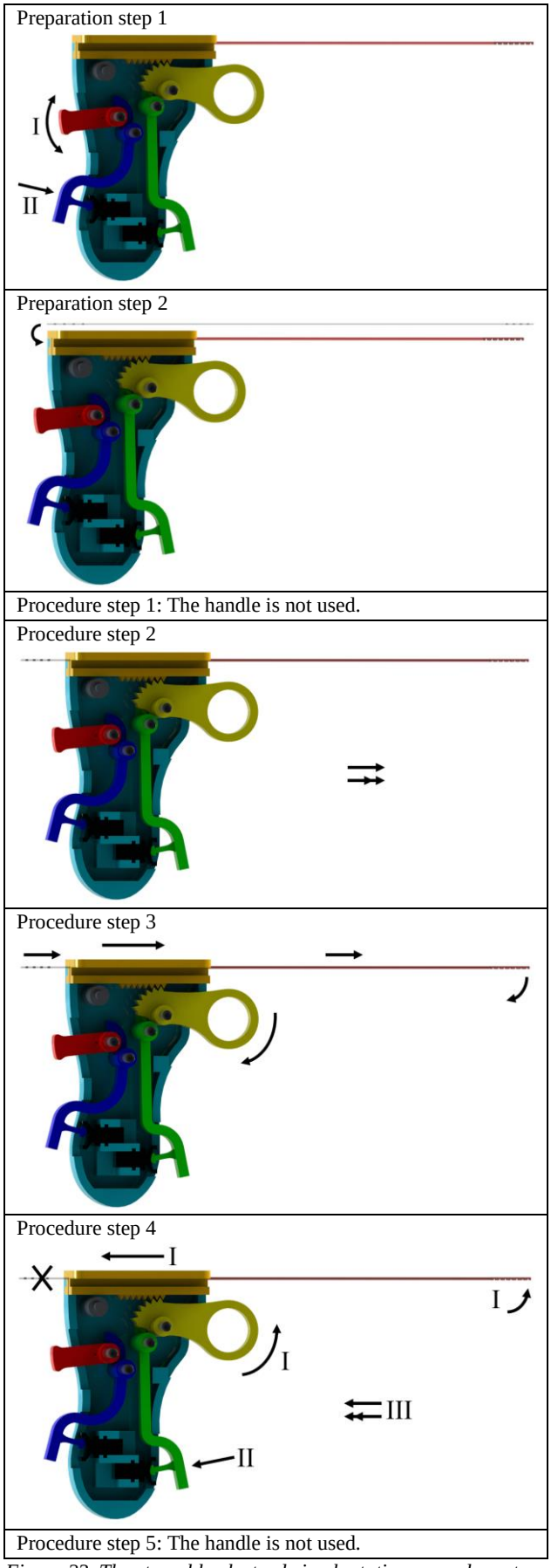

Figure 23. The steerable electrode implantation procedure steps that involve use of the handle. A cross means that the correspondent part is kept fixed during the step, an arrow means that the correspondent part is moved during that step. Double arrows indicate rotation around the axis of the arrow. Roman numbers indicate steps within steps.

5 Prototype

5.1 Manufacturing

The introduction shaft and the handle were manufactured separately. The proximal shaft end was made from a stainless-steel capillary tube, the distal end was made from plastic, and the steerable tip was made from a nitinol rod that was clamped between stainless-steel rings. Most of the handle parts were 3D-printed with PLA material, except for the lock catches and the screws and nuts. The lock catches were ordered from Brabantia [24], the attachment screws were machined from stainless-steel, and standard M5 nuts were used. Three rubber rings were added to provide more friction on the locks and to attach the pulling cable to the radius adjustment button.

5.1.1 Proximal and distal end of the shaft

The proximal end of the introduction shaft was 150 mm long and was cut from a stainless-steel capillary tube with an inner diameter of 1.4 mm and an outer diameter of 1.6 mm. The capillary tube was cut with pliers and then filed to remove the clamped end. Half of the circumference was filed out at one side over a length of 20 mm with a square miniature file to prevent rotation of the proximal end in the handle (Figure 24a).

The distal shaft end was an 80 mm long plastic shaft (Figure 24b). Conventional pre-curved introduction shafts are made from polyether ether ketone (PEEK) plastic, so the straight end of the conventional shaft could have been cut off and used for the prototype. However, no conventional shafts were available, so the plastic shaft was cut from another plastic tube. Unfortunately, the exact material of the plastic was not known, but it seemed to be similar to PEEK plastic. The inner and outer diameter of the plastic distal shaft end were 1.4 mm and 2.4 mm respectively. The outer diameter was larger than the design specifications because of a lack of correctly dimensioned shafts and to improve attachment to the prototype shaft tip, which also had a larger outer diameter. The plastic distal end was not perfectly straight, because of a lack of lateral elasticity and because the plastic shaft was delivered in a rolled-up form.

Figure 24. The proximal (a) and distal (b) shaft end of the prototype.

5.1.2 Shaft tip

The final steerable tip prototype was created by clamping a nitinol rod in between pieces of stainless-steel capillary tube (Figure 25). The nitinol rod had a diameter of 0.25 mm and the stainless-steel pieces of stainless-steel capillary tube had a 0.2 mm wall thickness and a 2.4 mm and 1.8 mm outer diameter, because of a lack of capillary tubes with smaller diameters that also had a diameter difference of 0.2 mm. Clamping the two capillary tube pieces over each other with the nitinol rod in between them deformed the walls of the capillary tube by 0.04 mm. A 300 mm long braided stainless-steel pulling cable with a diameter of 0.15 mm was attached to the opposite side of the nitinol rod in between the most distal stainless-steel rings with a knot. The cable ran through the other more proximal rings. The nitinol rod was 80 mm long and therefore had an additional 60 mm to attach the tip to the distal shaft end. The rings were cut off from the stainless-steel tube with electrode discharge machining and were clamped together with flat-nose pliers. The rings were placed on the nitinol rod with a precision of 0.04 mm with flat-nose pliers under a microscope with 50 times zoom. A 1.3 mm outer diameter rod was put inside the 1.8 mm outer diameter rings during clamping to prevent skew placement of the rod inside the rings. The rings had a width of 2.0 mm to provide enough friction and prevent translation rings over the nitinol rod. The final tip prototype had six rings next to each other. An earlier design with four rings had 4.0 mm in between the rings for a total ring distance of 20 mm. However, with 4.0 mm lateral slots, the force distribution was not equal over the length of all the rings and the distal end tended to bend less than the proximal tip end. To prevent unequal force distribution, the rings should touch each other in a fully bent state. Therefore, a tip design was made with six rings next to each other and a lateral slot width of 2.0 mm with a total length of the rings of 22 mm, as six rings was the maximum number of rings possible to reach the specified minimum radius of curvature.

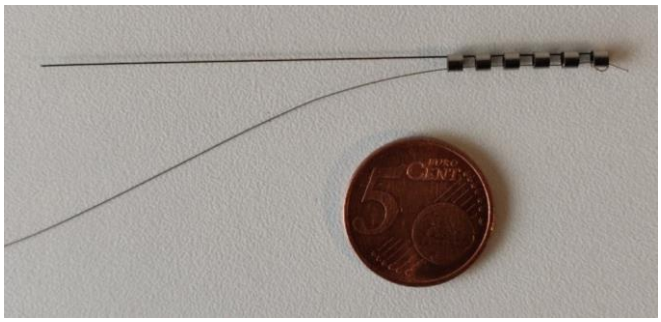

Figure 25. The final tip prototype consists of a nitinol rod with six stainless-steel rings next to each other and a braided stainless-steel cable that was attached to the most distal ring.

5.1.3 Handle

All the handle parts, except for the screws, nuts, and Brabantia lock catches, were printed using an Ultimaker 3 FDM 3D-printer (Figure 26). The designs were created in SolidWorks and saved as STL-files. The g-code of the STL-files was generated using the Ultimaker Cura 3.6.0 software. The parts were printed separately with PLA material with a print core of AA 0.4. All the default settings for the Ultimaker 3 were used and consisted of a layer height of 0.100 mm, 20% infill, with generated support and build plate adhesion. The combined printing time of all the components was 20 hours. The printer, just like other 3D-printers, did not print the parts with perfect precision. Therefore, the parts were sanded after printing P120 sanding paper, especially the holes for the screws and the surfaces of the support surfaces. Rubber rings with an 11 mm outer diameter and a 9 mm inner diameter were cut from the rubber on a BIC Intensity Gel pen [25]. The rubber rings were stretched around the circumference of the surface on the radius adjustment button and the bending trigger to increase friction of the locks on the corresponding button or trigger. The Brabantia lock catches were ordered from the Brabantia website [24] and standard M5 nuts were used. The screws were machined in the TU Delft 3ME workshop and were made from a 500 mm long stainless-steel solid shaft with a 9.0 mm diameter.

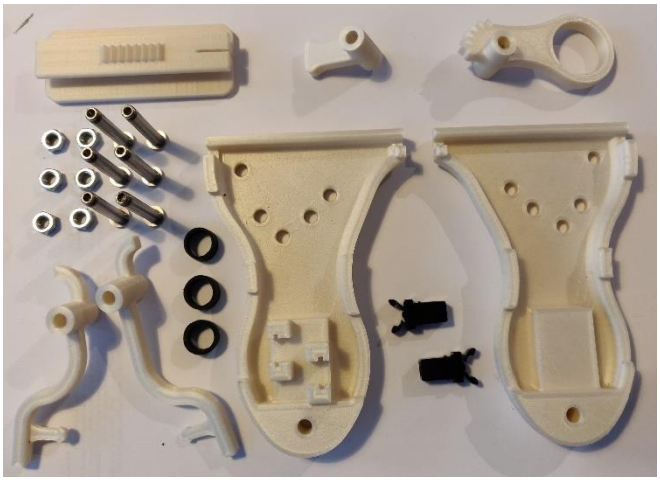

Figure 26. The 3D-printed handle parts (white) with the nuts and machined screws (silver), and the lock catches and rubber rings (black).

5.2 Assembly

The steerable shaft parts were assembled with shape-fits and a single layer of tape around the shaft parts (Figure 27a). A shrinking tube would have been a better solution, as the glue on tape is not biocompatible, but tape simplifies assembly and disassembly to experiment with different shaft tips. The plastic distal end was stretched over the stainless-steel proximal end over a length of 10 mm and was secured with a layer of tape. The extending nitinol rod of the steerable tip was positioned on the outside of the distal shaft and was secured with a single layer of tape over the nitinol rod and the distal end.

All the handle parts except for the rubber rings and the lock catches were locked inside the casing with the machined screws and the M5 nuts (Figure 27b). The rubber rings were stretched around the axes of the radius adjustment button and the bending trigger. The lock catches were fit inside the extruded shape in the middle of the casing (Figure 27c). The shaft assembly was shape-fitted inside the shaft rack to prevent rotation. The cable that was attached to the steerable tip was attached to the hole in the radius adjustment button next to its axis and was locked in between the axis and a rubber ring around the axis. The locked cable prevented translation of the shaft assembly inside the shaft rack. The shape fit of the shaft inside the shaft rack successfully prevented rotation of the proximal end of the shaft relative to the handle. The complete assembly had a width, length and depth of 282 mm, 120 mm, and 35 mm respectively.

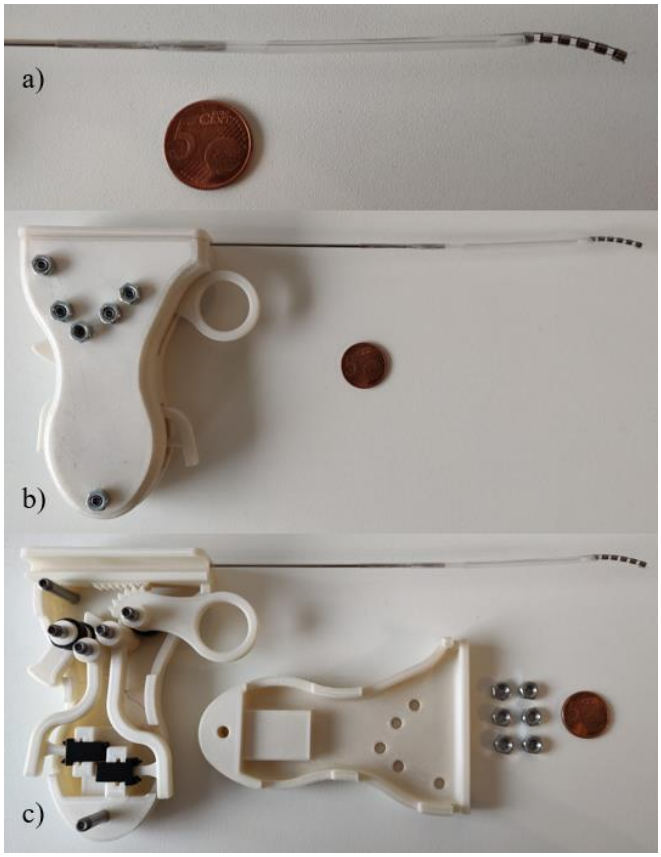

Figure 27. The prototype shaft assembly (a), the assembled prototype (b), and the prototype without the front casing part and nuts to show the inner components (c).

6 Proof of principle experiments

6.1 Experimental design, procedure, and data analysis

The working principle of the prototype was evaluated with four experiments. The experiments were organized considering the implantation steps that involve the use of the introduction shaft and the handle (Section 4.2.6).

1) *Steerable tip fatigue experiment.* The goal was to measure deformation of the steerable tip during a fatigue test (Section 6.1.1). The fatigue experiment was done first because the plastic deformation of the tip after bending could cause unpredictability in the rest of the experiments.
2) *First preparation step experiment.* The goal was to measure the required force to adjust the radius adjustment button, with and without the engagement of the corresponding locks (Section 6.1.2).
3) *Third and fourth procedure step experiment*. The goal was to measure the required force to adjust the bending trigger when pushing through epidural fat with and without engaging the bending trigger lock, the reached minimum radius of curvature of the steerable tip, the corresponding bending of the distal shaft end, and the potential intersection locations of the tip with the DRG (Section 6.1.3).
4) *Complete procedure experiment.* The goal was to determine the functioning of the prototype in comparison to the conventional implantation shaft by testing all the procedure steps consecutively in a mimicked spinal environment (Section 6.1.4).

6.1.1 Steerable tip fatigue experiment

Aim. The goal of the steerable tip fatigue experiment was to determine plastic deformation of the steerable tip after fully bending the tip multiple times. Specifically, the experiment was performed to find out if plastic deformation in the nitinol rod or translation of the stainless-steel rings over the nitinol rod would occur.

Variables. The measured variable was vertical displacement of the distal end of the tip in a relaxed straightened state. The radius adjustment button was kept in the bottom position to put the most stress on the steerable tip. The path of the bending trigger was kept constant and was moved from the top to the bottom position, as a full bend of the tip creates the most stress.

Setup. The setup consisted of the prototype, a measurement graph paper on a table, and a camera. The handle was positioned flat on the paper to measure the shape of the tip. A camera was used to make pictures of the tip on the measurement graph paper (Figure 28). Before the start of the experiment, a tip was assembled to the handle that had not been bent before. The bending trigger was set in the upwards position and the radius adjustment button was set in the downwards position.

Procedure. The initial vertical position of the tip was measured on the measurement graph paper. The steerable tip was bent 50 times from which the first ten bends were measured separately, and the rest of the bends were measured in steps of ten. Steps of ten were taken after ten bends to decrease experimenting time and look for a long-term result. A maximum number of 50 was chosen as none of the other experiments require the tip to bend more than 50 times. The experiment was conducted with the following steps. First, the bending trigger was moved from the top to the bottom position, and back to the top position. Second, a picture was taken of the tip on the measurement graph paper.

Data analysis. The pictures were analyzed by measuring the vertical position of the top of the shaft tip on the measurement graph paper. The vertical displacement was the vertical difference between the measured position of the distal end of the tip and the top of the proximal end of the tip. All the results were processed using Microsoft Office Excel 2016.

Figure 28. The setup of the steerable tip fatigue experiment consisted of measurement graph paper, a table, and a camera.

6.1.2 First preparation step experiment

Aim. The goal of the first preparation step experiment was to measure the required force to use the radius adjustment button with and without applying the radius adjustment button lock in the first preparation step.

Variables. The measured variable was the maximum force required to move the radius adjustment button. The maximum required force was measured over the whole travel of the button. The force was applied in a vertical direction at the middle of the circular shape on the button from the top of the button if moved downwards and from the bottom of the button if moved upwards. The independent variables were the path of the radius adjustment button, which was moved from top to bottom or from bottom to top, and the state of the radius adjustment button lock, which was applied or not applied.

Setup. The setup of the experiment consisted of the prototype, a bench vise, a table, and an analog push pull force gauge. The vise was locked to the side of the table. The handle was locked in a vertical position in the vise. The force gauge measures up to 10.0 N with a resolution of 0.05 N (Company and model: Sundoo SN-10) (Figure 29). The protruding flat-topped cylinder was attached to the pull screw on the force gauge and was applied to the bottom and top of the circular shape on the radius adjustment button to pull the button downwards from under the handle and upwards from above the handle respectively. The force gauge was reset and tuned in the to-be-measured position before every measurement. The electrode lead was not inserted in the shaft during this experiment, as the electrode lead is neither inserted in the first preparation step.

Procedure. The experiment was repeated ten times for all independent variables and was conducted with the following steps. First, the force gauge to 0.0 N with the force gauge was reset and tuned in a vertical upwards position. Second, the protruding cylinder of the force gauge was applied to the top of the radius adjustment button. Third, the maximum required force was measured to move the radius adjustment button downwards. Fourth, the force gauge was reset and tuned in a vertical downwards position. Fifth, the protruding cylinder of the force gauge was applied to the bottom of the radius adjustment button. The button was moved upwards slightly to facilitate applying the cylinder to the bottom of the button. Sixth, the maximum required force was measured to move the radius adjustment button upwards.

Data analysis. All the results of the force measurements were processed in Microsoft Office Excel 2016.

Figure 29. The setup of the first preparation step experiment consisted of a push pull force gauge (white), a bench vise (yellow), and a table.

6.1.3 Third and fourth procedure step experiment

Aim. The goal of the third and fourth procedure step experiment was to measure ergonomics of the bending trigger and steerable tip performance through epidural fat. The required force to use the bending trigger was measured when pushing through fat with and without applying the bending trigger lock. Steerable tip performance consisted of measuring the minimum radius and maximum angle of

curvature of the steerable tip using different settings of the radius adjustment button, maximum vertical displacement of the distal shaft end, and the tip path during the whole travel of the bending trigger to find optional intersections of the tip with the DRG.

Variables. The measured variables were the force on the spring scale, the vertical position of the end of the distal shaft end, the minimum radius and maximum angle of curvature of the tip, and the eventual intersections of the tip with the DRG over the whole trigger path. The travel of the bending trigger was kept constant and was moved from the top to the bottom position and back to the top position. The force was measured only with downwards motion of the trigger, as downwards motion requires more force than upwards motion because fat is pierced only during downwards bending trigger motion. The force was applied on the top of the circular hole on the trigger in a vertical downwards direction to resemble a downwards and towards the handle direction that the index finger makes when operating the handle. The independent variable was the position of the radius adjustment button, which was set to 0%, 50% or 100%. 0% Means that the button is in the upward position, 50% in the middle position, and 100% in the downward position.

Setup. The setup of the experiment consisted of the prototype, a bench vise, a table, an analog push pull force gauge, gelatin, a gelatin cube holder, a measurement graph paper with a resolution of 1 mm, a camera, and a plastic shaft (Figure 30). The vise was locked to the side of the table. The prototype handle was locked in an upwards vertical position in the vise and the plastic shaft was applied over the proximal shaft end to prevent proximal end bending. The plastic shaft was 105 mm long with a 2.5 mm inner diameter. The force gauge measures up to 10 N with a resolution of 0.05 N (Company and model: Sundoo SN-10). The protruding flat-topped cylinder was attached to the push screw on the force gauge and was applied to the middle of the top of the circular hole on the bending trigger in a vertical downwards direction. The gelatin cube holder and the gelatin box were laser-cut from transparent 2 mm thick PMMA. The gelatin cube holder was placed in front of the steerable shaft tip with the narrow side perpendicular to the shaft tip. The measurement graph paper was glued to the outside of the back of the gelatin cube holder. The camera was placed towards the grid 200 mm away from the gelatin cube holder. The gelatin box (60 x 200 x 200 mm) was used to create 40 gelatin cubes (20 x 50 x 50 mm). The gelatin box was removed from the refrigerator two hours before the start of the experiment to let the gelatin reach the room temperature, and the experiment was done within an hour afterwards. The gelatin cubes were cut out of the gelatin box with a kitchen knife and fit perfectly in the gelatin cube holder.

Gelatin samples preparation. The gelatin was prepared by mixing one part of gelatin powder with 20 parts of hot but not boiling water to achieve a 5% gelatin concentration, which resembles the density of human fat. The mixture was then put in the gelatin box, and the box was put in a refrigerator for at least four hours the day before the experiment. Proper mixing when the mixture was still hot was crucial to prevent having a thicker layer of gelatin at the bottom. Mixing when the mixture was getting colder and thus thicker created bubbles in the gelatin and deteriorated the view through the gelatin.

Procedure. The experiment was repeated five times for all independent variables and was conducted with the following steps. First, the bending trigger was set in the correct position. Second, a gelatin cube was inserted in the gelatin holder, and the holder was set in the correct position. Third, the hook of the force gauge was applied to the bending trigger. Fourth, the camera was turned on to start recording, while the force gauge was moved downwards, and the maximum force was measured. Fifth, the recording was stopped, and the video file was saved to a computer. Sixth, the gelatin cube was removed from the gelatin holder and the steerable tip was washed by dipping it in hot but not boiling water.

Data analysis. Measurements of the vertical distal end displacement, the tip radius of curvature, and the tip angle of curvature were made on a screenshot from the video file where the tip was fully bent. The vertical displacement of the distal shaft was measured by comparing the vertical location of the distal end of the distal end with the proximal end of the distal end. The minimum radius of curvature and maximum angle of curvature were measured by manually drawing a circle around the tip axis that resembled the shape of the bent tip. The circle was drawn on top of the screenshot using the Autodesk Sketchbook software. The radius of the drawn circle defined the tip radius of curvature. The angle of the tip was measured by comparing the distal tip end angle with proximal tip end angle (Figure 31). Potential tip intersections with the DRG where measured by looking at the shape of the bent tip and the translation of the tip when bending in the video file. The DRG was simulated on the grid in the recorded video to find possible intersections with the tip and the DRG size was set in correspondence with the reached minimum radius of curvature of the steerable tip. All the results were processed in Microsoft Office Excel 2016.

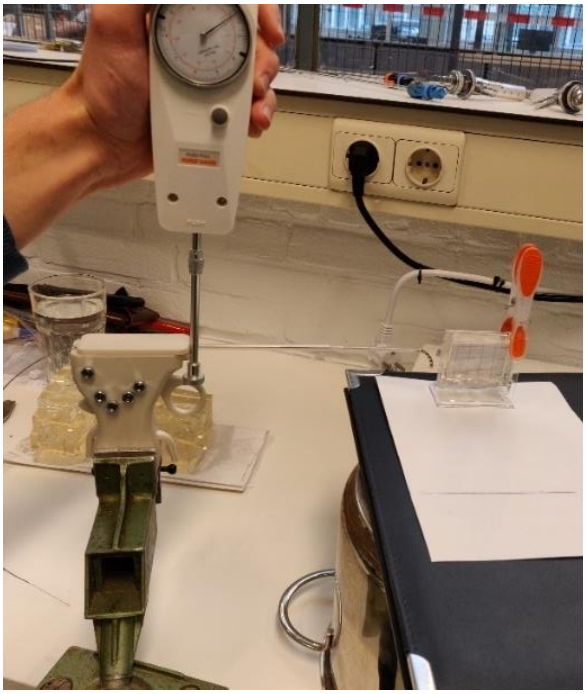

Figure 30. The setup of the third procedure step experiment consisted of a force gauge (white top), a bench vise (green), a table, and a gelatin holder (transparent with orange clip). The pan with the notebook on top was used to put the gelatin holder at the correct height. The paper on the blue notebook indicated the position of the gelatin holder and the camera phone with the blue stripes.

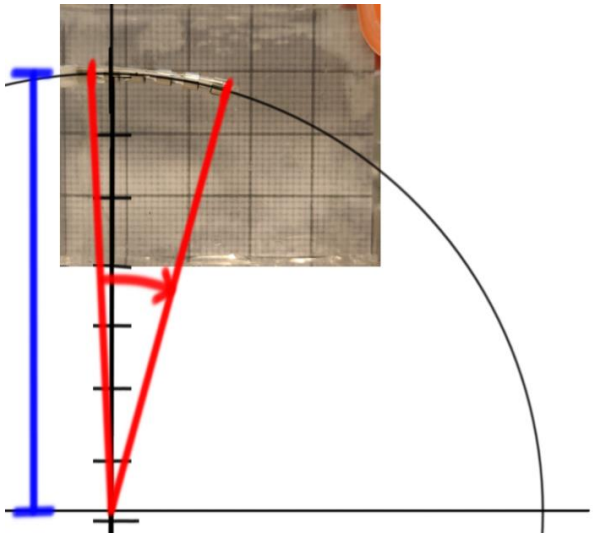

Figure 31. Measurement of the radius of curvature (blue) and the angle of curvature (red) of the steerable tip in the third and fourth procedure step experiment.

6.1.4 Complete procedure experiment

Aim. The goal of the complete procedure experiment was to determine the functioning of the prototype during all the implantation steps by implanting the electrode lead in a mimicked environment of the human lower spine.

Variables. Steerable tip performance was verified by measuring the percentage of the DRG circumference that was covered by the implanted electrode lead. The measured variable was the electrode lead coverage of the implanted electrode around the mimicked DRG. The DRG size was kept constant with a radius of 2.9 mm, as the DRG could then be mimicked with a standard M3 bolt.

Setup. The setup consisted of three artificial vertebrae surrounded by gelatin inside a transparent box, a 50 mm long M3 bolt, a table, and a plastic cutting board (Figure 32). The artificial vertebrae were three human-scaled [26] L3 lumbar vertebrae 3D-printed on top of each other. The L3 vertebra SolidWorks files were downloaded from the GrabCAD Community webpage [27] and were assembled in SolidWorks and printed with PLA material on an Ultimaker 3 3D-printer using the Cura 3.6.0 software with equal settings as in Section 5.1.3. The bolt was a 50 mm long M3 sized bolt that was glued laterally inside the intervertebral foramen between the two bottom vertebrae and served to mimic a DRG. The transparent box was made from laser-cut pieces of 2 mm thick PMMA and was placed around the vertebrae to hold the gelatin that mimicked the epidural fat. The gelatin was prepared in the box while a 1 kg metal cube was placed on top of the vertebrae to prevent floating in the gelatin mixture. See Section 6.1.3 for the description of the gelatin preparation. The gelatin box was carefully removed from the gelatin around the vertebrae two hours before the experiment to let the gelatin reach the room temperature. The vertebrae were placed with the spinous process upwards on the plastic cutting board. A camera was positioned about 200 mm away from the DRG and was held by another person to move the camera into different positions during the procedure.

Procedure. The experiment was done only once, because it was a qualitative test to verify if the implantation procedure was possible with the steerable introduction shaft. The experiment was conducted with the following steps. First, the electrode lead was implanted around the DRG without the Tuohy needle by entering the spine from the bottom in the spinal cord lumen while recording a video of the whole process. Second, a picture was taken of the implanted electrode result and the picture was uploaded with the recorded video to a computer. The steerable tip was not inserted through a Tuohy needle like in the implantation procedure but was inserted from the bottom of the bottom vertebra straight into the lumen of the spinal cord. The Tuohy needle was not used as it complicated the experiment without adding value and because of a lack of appropriately sized Tuohy needles for the steerable tip prototype.

Data analysis. The angle of curvature of the electrode lead was measured by manually drawing a circle around the lead on the picture and comparing the angle of the proximal and distal lead ends on the circle. The circle was drawn on top of the picture using the Autodesk Sketchbook software. The DRG electrode lead coverage was calculated by comparing the angle of curvature of the lead with a full circle.

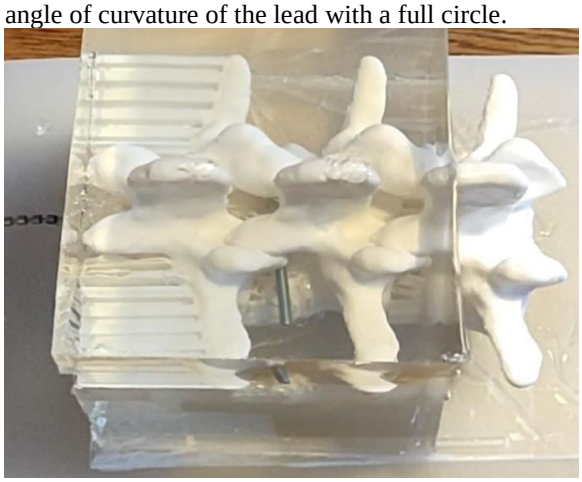

Figure 32. The complete procedure experiment setup consisted of three L3 spinal vertebrae 3D-printed on top of each other surrounded by gelatin. The steerable tip was inserted into the spinal cord lumen from the bottom of the vertebrae and aimed to surround the M3 bolt that mimics the DRG. The vertebrae were positioned on a plastic cutting board on top of a table.

7 Results

7.1 Steerable tip fatigue experiment

The goal of the steerable tip fatigue experiment was to measure deformation of the steerable tip during a fatigue test. Detached from the handle, the steerable tip showed no signs of fatigue after bending the tip multiple times. Attached to the handle, the steerable tip initially remained bent 0.4 mm in a relaxed state. After bending the tip more than once at the lower radius adjustment button setting without the electrode lead inside it, the tip remained bent 2.4 ± 0.3 mm (mean ± standard deviation) vertically at the distal end of the tip (Figure 33). An upward trend with a small slope was seen after bending the tip more than once.

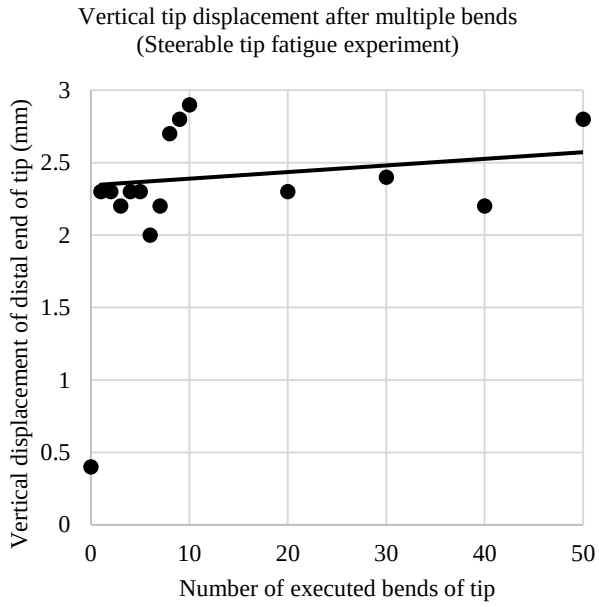

Figure 33. Scatter plot of the vertical displacement of the distal end of the steerable tip to measure plastic deformation of the tip in the steerable tip fatigue experiment.

7.2 First preparation step experiment

The goal of the first preparation step experiment was to measure the required force to adjust the radius adjustment button, with and without the engagement of the corresponding locks. The lock catches could be applied with any position of the respective to-be-locked button and is thus a continuous locking mechanism. The maximum required force to move the radius adjustment button in the first preparation step without applying the corresponding lock catches was 1.05 ± 0.06 N (mean ± standard deviation) when moving the button downwards, and 1.10 ± 0.13 N when moving the button upwards (Figure 34).

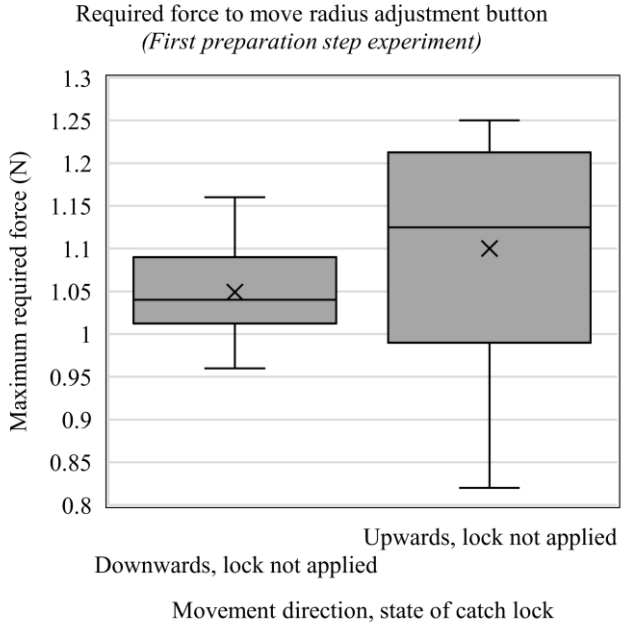

Figure 34. Box plot of measured data of the maximum required force to move the radius adjustment button without applying the radius adjustment lock and without an inserted electrode lead in the first preparation step experiment. Gray boxes represent results between the top and bottom quartile with a black stripe for the median and a cross for the mean.

The maximum required force to move the radius adjustment button in the first preparation step with the radius adjustment lock applied was 6.73 ± 0.26 N when moving the button downwards, and 8.78 ± 0.36 N when moving the button upwards (Figure 35). Consequently, the lock substantially increased the friction on the button six to nine times. The lock increased the friction more when the button was moved upwards than when the button was moved downwards.

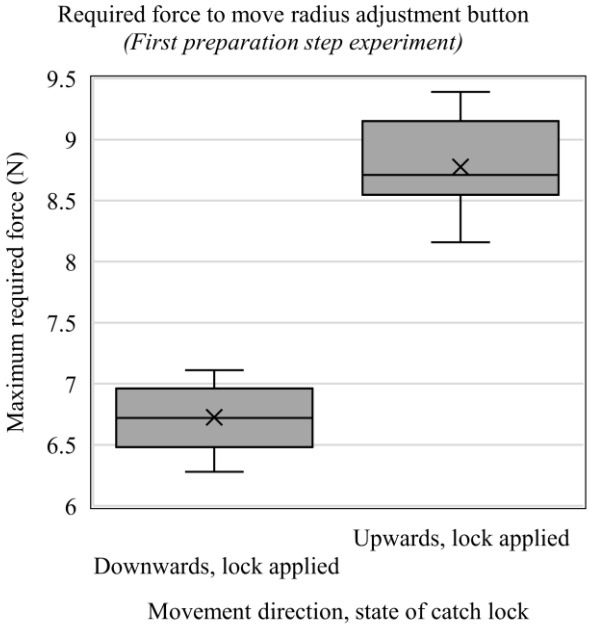

Figure 35. Box plot of measured data of the maximum required force to move the radius adjustment button with the radius adjustment lock applied and without an inserted electrode lead in the first preparation step experiment. Gray boxes represent results between the top and bottom quartile with a black stripe for the median and a cross for the mean.

7.3 Third and fourth procedure step experiment

The goal of the third and fourth procedure step experiment was to measure the required force to adjust the bending trigger when pushing through epidural fat with and without engaging the bending trigger lock, the reached minimum radius of curvature of the steerable tip, the corresponding bending of the distal shaft end, and the potential intersection locations of the tip with the DRG. The maximum required force to move the bending trigger when pushing the steerable tip through gelatin without applying the lock was 1.83 ± 0.17 N, 2.25 ± 0.46 N, and 2.70 ± 0.30 N (mean ± standard deviation) with a radius adjustment button at 0%, 50%, and 100% respectively (Figure 36). The bending trigger movement force increased slightly with lower positions of the radius adjustment button.

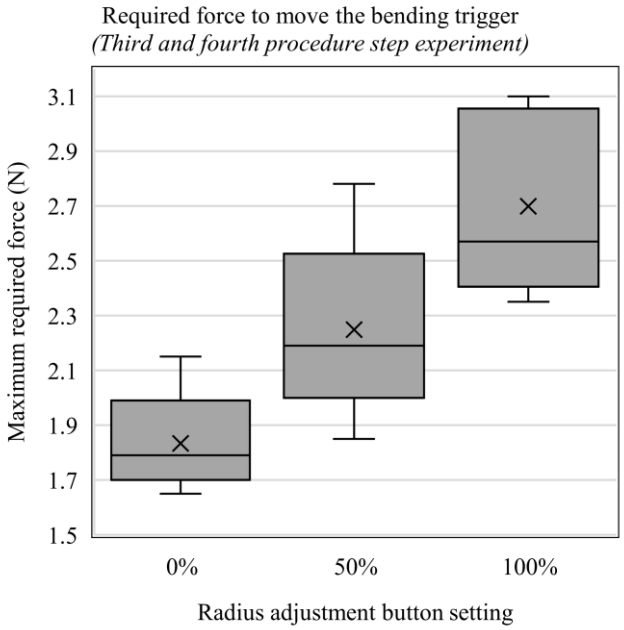

Figure 36. Box plot of measured data of the maximum required force to move the bending trigger when pushing the steerable tip through gelatin in the third and fourth procedure step experiment. Gray boxes represent results between the top and bottom quartile with a black stripe for the median and a cross for the mean.

Detached from the handle, the steerable tip reached the specified 3.0 mm minimum radius of curvature. Attached to the handle, the steerable tip reached a radius of curvature of 42 ± 14 mm, 13 ± 1 mm and 6 ± 1 mm (Figure 37) with a radius adjustment button setting of 0%, 50% and 100% respectively. The minimum radius of curvature with the lowest radius adjustment button setting was 3 mm too large compared to the specified minimum radius of curvature of 3.0 mm. The setting of the radius adjustment button also showed a non-linear relation with the reached radius of curvature, and the range between the minimum and maximum radius of curvature was too large compared to the specified range between 3.0 and 6.5 mm.

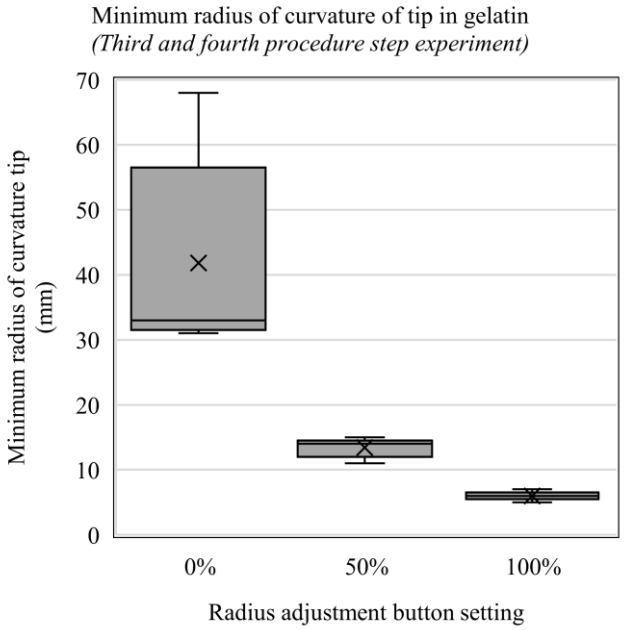

Figure 37. Box plot of measured data of the minimum radius of curvature of the steerable tip in the third and fourth procedure step experiment. Gray boxes represent results between the top and bottom quartile with a black stripe for the median and a cross for the mean.

Attached to the handle, the steerable tip reached an angle of curvature of 34 ± 8˚, 83 ± 6˚ and 185 ± 4˚ (Figure 38) with a radius adjustment button setting of 0%, 50% and 100% respectively. Accordingly, the tip reached a maximum circumference percentage of 51.4 ± 1.1%, which is more than double the circumference reached with conventional implantation shafts.

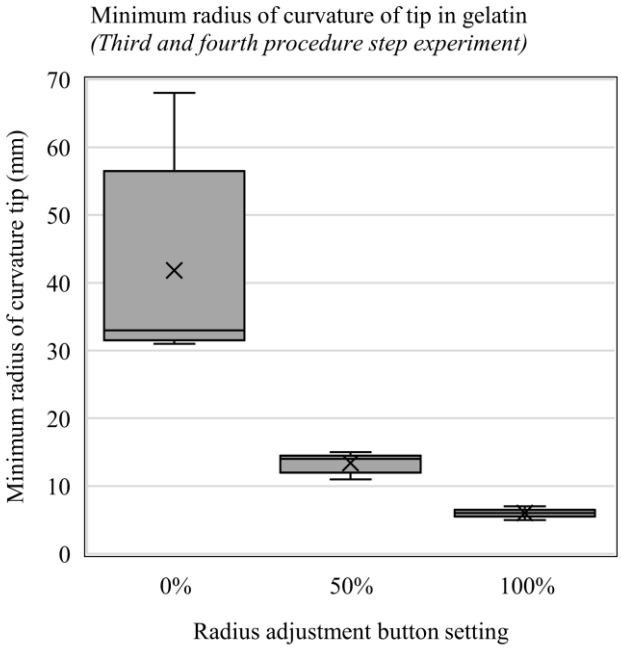

Figure 38. Box plot of measured data of the maximum angle of curvature of the steerable tip in the third and fourth procedure step experiment. Gray boxes represent results between the top and bottom quartile with a black stripe for the median and a cross for the mean.

The proximal and distal shaft ends did not deform vertically when the steerable tip was bent completely inside the gelatin. The steerable tip always bent with a circular path or with a path slightly less curved than a circle (Figure 39). The tip did intersect with the simulated DRG on the recorded videos as the shaft rack lacked about 8 mm of translation in relation to tip bending.

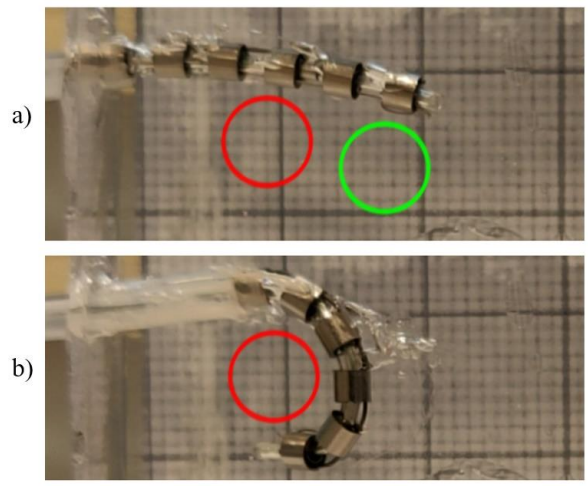

Figure 39. The steerable tip in the straight (a) and fully bent (b) position. The green circle represents a proper DRG position around which the tip should have bent optimally. The red circle represents a DRG position around which the current prototype would bend correctly. The distance between the circles shows that

the tip lacked translation during bending. The tip entered the gelatin at a small angle because the plastic distal shaft end was not perfectly straight.

After implanting the electrode lead inside the gelatin, the electrode lead straightened slightly (Figure 40). The radius of curvature difference between the steerable tip and the correspondent implanted electrode lead were 15 ± 11 mm, 7 ± 2 mm, 2 ± 0 mm (Figure 41) with a radius adjustment button setting of 0%, 50%, and 100% respectively.

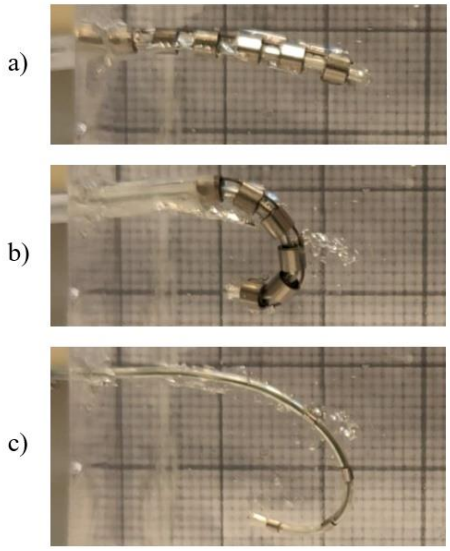

Figure 40. The electrode lead inside a straight steerable tip (a), a fully bent steerable tip (b), and inside the gelatin after extracting the steerable tip (c).

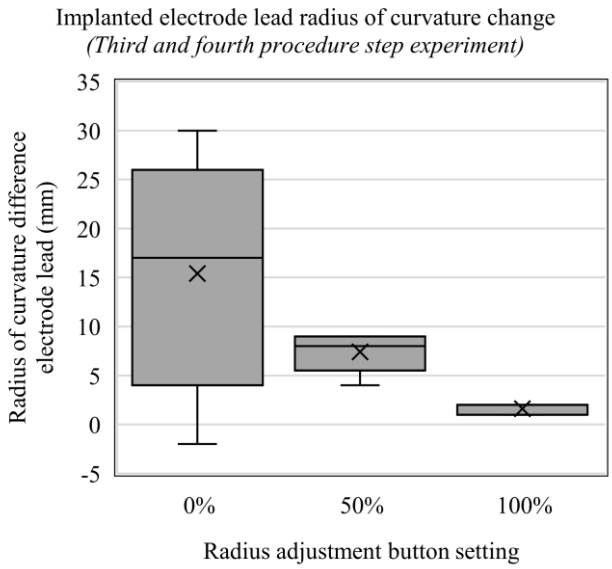

Figure 41. Box plot of measured data of the radius of curvature difference of the implanted electrode lead after implantation in gelatin in the third and fourth procedure step experiment. Gray boxes represent results between the top and bottom quartile with a black stripe for the median and a cross for the mean.

The angle of curvature difference between the steerable tip and the correspondent implanted electrode lead were 11 ± 5˚, 37 ± 5˚, 57 ± 23˚ (Figure 42) with a radius adjustment button setting of 0%, 50%, and 100% respectively.

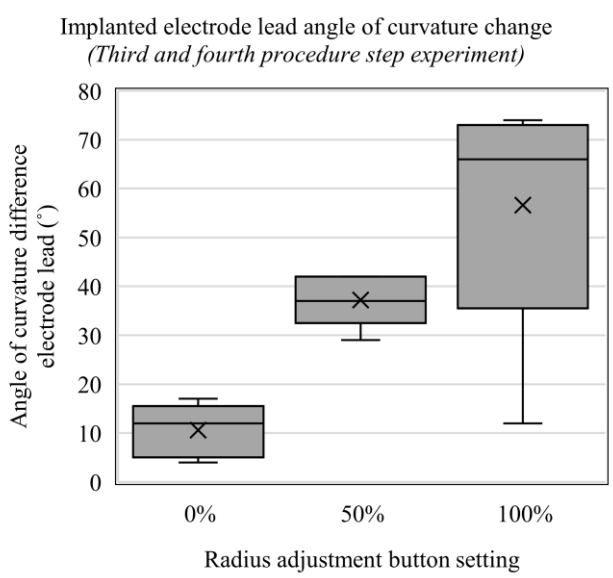

Figure 42. Box plot of measured data of the angle of curvature difference of the implanted electrode lead after implantation in gelatin in the third and fourth procedure step experiment. Gray boxes represent results between the top and bottom quartile with a black stripe for the median and a cross for the mean.

7.4 Complete procedure experiment

The goal of the complete procedure experiment was to determine the functioning of the prototype in comparison to the conventional implantation shaft by testing all the procedure steps consecutively in a mimicked spinal environment. In the complete procedure experiment, an electrode lead was successfully implanted in artificial 3D-printed vertebrae surrounded by gelatin (Figure 43). The achieved electrode array DRG circumference coverage was roughly 50%, which is 25% more than the potential coverage of conventional introduction shafts. The radius of curvature of the electrode lead was larger than expected and the lead was positioned about 4 mm away from the M3 bolt at some parts of the circumference, while the lead should have been positioned about 1 mm away from M3 bolt.

Figure 43. The implanted electrode lead around an M3 bolt (green circle) that mimicked a DRG in the intervertebral foramen of a 3D-printed vertebrae surrounded by gelatin.

8 Discussion

8.1 Design

The final design of the steerable electrode lead introduction shaft is shown in Figure 16. The shaft has an inner lumen the electrode lead and consists of a proximal end, a distal end, and a steerable tip. The steerable tip can bend in one direction and consists of stainless-steel rings clamped on a nitinol rod. The

shaft is connected to a handle that provides control of the shaft during the implantation procedure. A pulling cable is attached to the distal end of the tip and the radius adjustment button inside the handle. The radius adjustment button allows for adjustment of the minimum radius of curvature that the tip can achieve. The bending trigger in the handle can be used to translate the shaft forward and bend the tip. The radius adjustment button and the bending trigger can be locked separately in any position with additional lock buttons. The shaft design is innovative in terms of shaft maneuverability, as the shaft tip can be moved in a circular path around the DRG by combining shaft translation and tip bending. The electrode lead can be released by pushing the lead through the shaft, even when the tip is bent. After completing all the experiments and receiving feedback from a neurosurgeon, it was confirmed that the handle has a comfortable size and grip to perform all the necessary steps in the electrode implantation procedure. Compared to conventional pre-curved introduction shafts, the steerable introduction shaft decreases the minimum radius of curvature of implanted electrode leads around the DRG from 15 mm to 6 ± 1 mm and increases the maximum angle of curvature from 90˚ to 185 ± 4˚. Several aspects of the design can be improved in a later design iteration to improve the results of the experiments. Optimizations include changes to the radius adjustment button, the bending trigger, the shaft rack and the steerable tip (Figure 44).

The tip stays slightly bent after fully bending the tip and letting the tip relax. An explanation is that friction between the pulling cable and components inside the shaft and the handle keep residual stress on the pulling cable. The slightly bent tip can be straightened manually by applying an external force on the tip in the opposite direction of the bend or by inserting the electrode lead including the internal nitinol rod into the shaft. Therefore, incomplete straightening of the tip is not a disadvantage for the implantation procedure, as the electrode lead is inserted into the tip in the second preparation step. However, the tip does stay slightly bent even when inserting the electrode lead, but not enough to prevent straight movement through epidural fat. The residual stress that stays in the pulling cable can be minimized by giving the internal slope inside the shaft rack an even more circular shape to prevent sharp angles and reduce friction on the pulling cable. The screw that guides the pulling cable can also be decreased in size to decrease the area of the screw that is in contact with the pulling cable. The slope in the shaft rack and screw that guide the pulling cable are the only parts of the handle that create friction on the pulling cable, except for the internal wall of the shaft. The friction on the cable can be minimized further by lubricating the cable in oil or a thin layer of Teflon. The friction between the other moving components can also be decreased with a dry lubricant to decrease the required force to move the radius adjustment button and the bending trigger.

The minimum radius of curvature of the steerable tip is adjustable between 42 ± 14 mm and 6 ± 1 mm compared to the specified 6.5 and 3.0 mm. The range between the minimum and maximum radius of curvature of the steerable tip can be decreased by decreasing the length difference that the radius adjustment button inflicts on the pulling cable. The cable length difference can be decreased by either decreasing the range of the button or by decreasing the distance between the pulling cable attachment hole and the button axis. As the radius adjustment button shows a non-linear relation with the reached radius of curvature of the steerable tip, once the range of the button is adjusted, the reached radius of curvature of the tip related to every position of the button can be experimentally verified to find the optimal button setting for different DRG sizes. The minimum radius of curvature of the steerable tip can be decreased by increasing the movement range of the bending trigger or by increasing the diameter of the gear on the bending trigger. The pulling cable can also be attached tighter to the radius adjustment button to decrease the minimum radius of curvature. However, a larger movement range of the bending trigger results in a straightened tip even when the bending trigger is moved downwards slightly, and a tighter cable results in a slightly bent tip even when the bending trigger is set to the top position.

The steerable tip does not make a perfect circular motion when using the bending trigger, as the shaft does not translate sufficiently. A manual solution to increase translation of the shaft rack is to position the middle of the tip instead of the distal end of the tip at the distal side of the DRG before using the bending trigger in the second procedure step, as the tip then surrounds the DRG without intersecting with it. Shaft translation can also be increased by increasing the size of the bending trigger gear to increase the translation range of the shaft rack and to leave some spare pulling cable length when the bending trigger is set to the top position. Accordingly, the steerable tip translates more by using the bending trigger and starts bending at a lower position of the trigger. A more radical design change to increase shaft rack translation is discussed in the future work Section 8.4.

The electrode lead fit inside the shaft and slid through the shaft easily upon insertion. The electrode lead was inserted through the back of the shaft rack all the way to the distal end of the shaft tip with translation and rotation of the lead relative to the introduction shaft. When the steerable tip was fully bent, the electrodes on the electrode array tended to cling to the stainless-steel rings of the steerable tip upon retraction of the electrode lead through the shaft. Clinging of the electrodes to the steerable tip was minimized by slightly rotating the electrode lead upon retraction, and the electrode lead was successfully implanted in the gelatin cubes. Clinging of the electrodes on the electrode lead to the stainless-steel rings of the steerable tip upon retraction of the electrode lead through the shaft can be decreased by decreasing the width and increasing the number of stainless-steel rings in the tip, and by subsequently decreasing the gap width in between the rings. The stainless-steel rings also should be scaled down to meet the design specifications, but this topic is discussed further in the future work Section 8.4.

Some prototype characteristics found in the test phase did not require design optimizations as they did not pose disadvantages for the implantation procedure. The radius adjustment lock increased the friction more when the radius adjustment button was moved upwards than when the button was moved downwards. This might be caused by gravity or a measurement difference between the push- or pull configuration of the push-pull force gauge. However, no design optimizations are needed as the lock increases the friction sufficiently in both the upwards and the downwards direction. The proximal and distal shaft ends did not deform vertically when the steerable tip was bent completely inside the gelatin, as the gelatin provided an external force in the opposite direction of the downwards force of the pulling cable on the steerable tip. Consequently, the stiffness of the distal shaft end does not have to be increased.

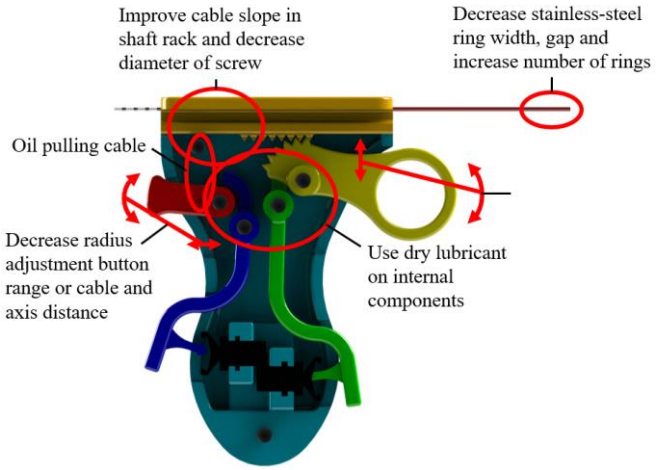

Figure 44. The steerable introduction shaft and handle with design optimization recommendations to improve performance of the steerable introduction shaft.

8.2 Experimental design

The experiments proved the working principle of the prototype, but the experimental design can be improved to decrease the standard deviation in the results.

In the steerable tip fatigue experiment, an upward trend with a small upwards slope was seen even after bending the tip more than once. However, the tip straightened again after detaching the tip from the handle meaning that the tip did not deform plastically. Therefore, the upwards slope could have been caused by irregular straightening of the tip or by unprecise measurements in the experiment. The setup of the steerable tip fatigue experiment can be improved by attaching the distal end to the measurement graph paper to prevent having irregular positions of the tip on the paper.

The first preparation step experiment can be improved by measuring the required maximum force on the radius adjustment button and bending trigger with a more precise and smaller measuring device. The used force gauge is too large and heavy to be held comfortably, and a restriction of space during the experiment requires holding the device in a slightly tilted instead of vertical manner, diminishing the precision of the force reading. This also counts for the third and fourth procedure step experiment.

In the third and fourth procedure step experiment, the minimum radius of curvature difference between a tip with an inserted electrode lead and a tip without an inserted electrode lead was not tested because the tip is never bent without an inserted electrode lead in the implantation procedure. However, the minimum radius of curvature did seem to increase slightly when inserting the electrode lead. Therefore, adding another test without an inserted electrode lead can result in insights on how much the electrode leads influences the maximum radius of curvature of the tip. The thickness of the gelatin cubes in the gelatin holder can be reduced to decrease distortion of the view through the gelatin to measure the tip curvature on the measurement graph paper behind the gelatin holder. The gelatin boxes can be improved by finding a way to get rid of the slits in between the fitting pieces of the boxes. The used boxes out of laser-cut PMMA pieces have the correct dimensions, but the slits in between the fitting pieces do not retain the liquid gelatin mixture in the box, letting the gelatin drip out slowly when cooling it down in the refrigerator. As a solution, plastic boxes can be made in a mold. This also counts for the complete procedure experiment.

In the complete procedure experiment, the electrode lead was successfully implanted around the DRG even with the larger than specified outer diameter of the shaft and the clinging of the electrodes to the steerable tip that prevented the electrode lead to be released in a fully bent state. However, the mimicked environment of the spine was simplified compared to a real human spine. The spinal cord and the motor nerves were absent, and the epidural fat in the human spine contains arteries and vessels. The procedure was also simplified by excluding the first procedure step and the insertion of the Tuohy needle.

In the future, the experiments can be repeated more times to improve the data of the experiments, as the first preparation step experiment and the third and fourth procedure step experiment were repeated five times per independent variable, and the complete procedure experiment was done once. However, before doing so, the prototype should be optimized with the design optimizations stated in Section 8.1 and the future design changes stated in Section 8.4.

8.3 Challenges

Some challenges in the electrode lead implantation procedure cannot be solved by improving the introduction shaft. Other instruments should be improved as well to perfect the implantation procedure.

The stiffness of the implanted electrode lead is large enough to make the lead straighten slightly in the gelatin after implantation as discussed in Section 7.3. The steerable tip cannot make up for the extra displacement of the lead by decreasing the minimum radius of curvature, as the tip would then intersect with the DRG and damage it. The stiffness in the electrode lead is either caused by the material of the lead or the internal cables that connect the proximal and distal electrode array. The manufacturing of a more flexible electrode lead would be a solution to this problem.

Imaging of both the introduction shaft and the electrode lead during the procedure stays a challenge. Currently, both devices are imaged with fluoroscopy, creating a discontinuous image with health risks for both the patient and the doctors because of radiation. The steerable shaft can be imaged with fluoroscopy, as it is made from metals only. However, better yet undiscovered imaging techniques with continuous output and with less radiation could improve the use of the steerable introduction shaft even more.

8.4 Future work

In the future, apart from design optimizations as stated in Section 8.1, more drastic design changes can be made to improve the steerable electrode introduction shaft further. Recommended design changes for the shaft (Figure 45) are the downscaling of outer diameter of the steerable tip from 2.4 mm to 1.6 mm and replacing the distal end by a spring. Recommended design changes for the handle (Figure 46) are a lock mechanism between the pulling cable and the radius adjustment button, repositioning of the radius adjustment button with the corresponding lock, and hiding the nuts in the casing. Additions are a Luer lock to prevent translation of the electrode lead relative to the handle and to provide equal lead translation to shaft retraction in the fourth procedure step. Finally, a redesign of the internal bending trigger, shaft rack, and shaft tip can be made to adapt the steerable tip length while keeping a constant angle of curvature when longer electrode arrays become available.

The outer diameter of the steerable tip can be scaled down from 2.4 mm to the 1.6 mm as stated in the design specifications. Subsequently, the stainless-steel rings as well as the nitinol rod should become smaller. Every time the design becomes smaller, the friction of the stainless-steel rings on the nitinol rod should be experimentally verified to see if the pulling cable causes translation of the rings over the nitinol rod.

The plastic distal end can be replaced with a metal spring design. The spring-like shape gives the distal end lateral flexibility to bend through the bevel-tip of the Tuohy needle and axial stiffness to push through the epidural fat. The lateral elasticity of the spring also improves straightening of the distal end compared to a plastic shaft. A metal distal end with a spring-like shape makes sure that the whole shaft assembly is made from metal, providing better and more rigid attachment techniques between the proximal and distal end and the steerable tip by means of soldering or welding. Accordingly, the entire shaft assembly could be machined out of a single nitinol rod or tube. The use of a shrinking tube instead of tape can also be verified if the plastic rod is not replaced by a spring to connect the distal end to the tip, as tape is not biocompatible.

Future changes to the handle can optimize the functioning of the introduction shaft further as well. Shaft translation in relation to tip bending should be increased to improve the circular motion of the tip around the DRG. One way to decrease tip bending in relation to shaft translation when using the bending trigger is by adding a translational DOF to the screw that stretches the pulling cable above the radius adjustment button. A hole can be made in the casing to allow screw translation, and a spring can be added in this hole to make sure the pulling cable is stretched sufficiently. An extra cable can be attached between the screw and the bending trigger to allow lateral movement of the screw when bending the tip with the bending trigger. Consequently, the tip bends less while the shaft translates equally, as more travel of the pulling cable is needed to bend the tip. The gear diameter of the bending trigger and the length of the rack on the shaft rack can then be increased to increase translation and bending.

An adjustable locking mechanism can be designed to attach the pulling cable to the radius adjustment button, as the attachment of the pulling cable with the exact cable tightness is cumbersome. The locking mechanism can consist of a metal square with one hole to let the cable through and a lateral threaded hole to insert a screw that can be screwed in to lock the cable in the square. These locking mechanisms can also be used to attach the extra cable between the translational screw and the bending trigger mentioned in the previous paragraph.

The handle can be visually optimized by adjusting the casing to hide the nuts in notches and by giving the casing a more rounded shape to fit the hand even more comfortably. The radius adjustment button and radius adjustment button lock can be decreased in size or repositioned on the top of the handle instead of on the back to prevent the protruding components to interfere with the palm of the hand. The buttons can be positioned on the top as they are only used in the first preparation step when the handle can be used with two hands.

A Luer lock is used on the conventional introduction shaft to lock the electrode lead in the shaft to prevent relative translation of the lead in the shaft. The steerable introduction shaft has no lock to prevent translation of the electrode lead, as the shaft assembly already provides enough friction on the lead to prevent relative translation. However, if the shaft assembly has less friction on the lead in further design iterations, a Luer lock can be applied at the proximal end of the shaft rack. The Luer lock can then also be used to provide equal lead translation upon shaft retraction in the fourth procedure step if the lock is attached to the casing. Currently, with the steerable shaft as well as the conventional introduction shaft, lead translation through the shaft is done manually. However, it is crucial that the lead is translated forward equally when the shaft is retracted backwards to prevent pulling the electrode lead away from the surrounded DRG. Locking the lead to the casing when translating the shaft rack backwards with the bending trigger makes sure that the electrode lead stays in place around the DRG, while the shaft tip retracts back to the dorsal area of the DRG. However, forward lead translation when fully retracting the shaft through the needle once the shaft tip is straightened completely should still be done manually.

Finally, if an electrode lead with more than four contact points and a wider electrode array become available, a complete redesign of the shaft, bending trigger gear and shaft rack pinion mechanism can be made to make sure that the steerable tip has a constant maximum angle of curvature and an adjustable minimum radius of curvature to surround any DRG size with the same circumference percentage. To differ the radius of curvature with a constant angle of curvature, the mechanism should have an adaptive steerable tip length to increase and decrease the implanted electrode array length for relatively larger and smaller DRGs respectively. With a full DRG circumference coverage, electrodes that undesirably stimulate the motor nerve next to the DRG can then be switched off to always have desirable neurostimulation on a full circumference of 360˚.

Figure 45. Drawing of a metal spring distal shaft end design with a scaled down shaft tip with more and thinner stainless-steel rings.

Figure 46. Redesign of the handle with a spring to allow lateral movement of the pulling cable axis, three cable locks (purple), and a Luer lock (pink) that is attached to the rear casing part (light blue). The Luer lock has a proximal button to engage the lock. The radius adjustment button (red) is shortened. An extra pulling cable (red, right) is added between the bending trigger and the axis of the other pulling cable (red, left).

9 Conclusion

A prototype of a minimally-invasive steerable electrode lead introduction shaft was designed to improve DRG neurostimulation by decreasing the minimum radius of curvature and increasing the angle of curvature of implanted electrode leads around DRGs. The steerable shaft tip has a length of 22 mm with an outer diameter of 2.4 mm and consisted of clamped stainless-steel rings on a nitinol rod. An internal braided stainless-steel pulling cable was attached to the distal ring to bend the tip with a single degree-of-freedom in one direction. An ergonomic handle (120 x 75 x 35 mm) provided shaft rotation and translation, minimum radius of curvature adjustment, and combined shaft translation and tip bending. The prototype was tested to verify functioning and ergonomics in the implantation procedure steps that involve the use of the handle. The steerable tip reached a DRG circumference coverage of 51.4 ± 1.1% compared to a 25% potential coverage of conventional introduction shafts. The minimum radius of curvature was adjustable between 42 ± 14 mm and 6 ± 1 mm, compared to a specified adjustable range between 3.0 and 6.5 mm and a minimum radius of curvature of 15 mm of conventional introduction shafts. An electrode lead was successfully implanted in 3D-printed vertebrae surrounded by gelatin. In the future, the outer diameter of the prototype tip should be decreased to reach the required size for the procedure (1.6 mm), and the handle should contain a mechanism to increase shaft translation relative to the tip bending in order to improve circular motion of the steerable tip.

References

[1] K. L. Moore, A. F. Dalley, and A. M. R. Agur, *Clinically oriented anatomy*. Lippincott Williams & Wilkins, 2013.

[2] A. Siegel and H. N. Sapru, *Essential neuroscience*. Lippincott Williams & Wilkins, 2006.

[3] G. Kayalioglu, "The Spinal Nerves," in *The Spinal Cord*San Diego: Academic Press, 2009, pp. 37-56.

[4] M. Zimmermann, "Pathobiology of neuropathic pain," *European Journal of Pharmacology*, vol. 429, no. 1, pp. 23-37, 2001.

[5] B. H. Smith and N. Torrance, "Epidemiology of neuropathic pain and its impact on quality of life," *Current Pain and Headache Reports*, vol. 16, no. 3, pp. 191-198, 2012.

[6] K. E. Matzel *et al.*, "Sacral neuromodulation: Standardized electrode placement technique," *Neuromodulation: Technology at the Neural Interface*, vol. 20, no. 8, pp. 816-824, 2017.

[7] M. J. A. Malessy and W. Pondaag, "Neonatal Brachial Plexus Palsy with Neurotmesis of C5 and Avulsion of C6: Supraclavicular Reconstruction Strategies and Outcome," *JBJS*, vol. 96, no. 20, p. e174, 2014.

[8] J. Shen, H.-Y. Wang, J.-Y. Chen, and B.-L. Liang, "Morphologic Analysis of Normal Human Lumbar Dorsal Root Ganglion by 3D MR Imaging," *American Journal of Neuroradiology*, vol. 27, no. 10, pp. 2098-2103, 2006.

[9] E. Vialle, L. R. Vialle, W. Contreras, and C. Jacob Junior, "Anatomical study on the relationship between the dorsal root ganglion and the intervertebral disc in the lumbar spine," *Revista Brasileira de Ortopedia*, vol. 50, pp. 450-454, 2015.

[10] M. P. Silverstein, L. J. Romrell, E. C. Benzel, N. Thompson, S. Griffith, and I. H. Lieberman, "Lumbar Dorsal Root Ganglia Location: An Anatomic and MRI Assessment," *International Journal of Spine Surgery*, vol. 9, p. 3, 2015.

[11] M. S. Cohen, E. J. Wall, R. A. Brown, B. Rydevik, and S. R. Garfin, "1990 AcroMed Award in basic science. Cauda equina anatomy. II: Extrathecal nerve roots and dorsal root ganglia," (in eng), *Spine*, vol. 15, no. 12, pp. 1248-1251, 1990.

[12] T. Vancamp, R. M. Levy, I. Pena, and A. Pajuelo, "Relevant anatomy, morphology, and implantation techniques of the dorsal root ganglia at the lumbar levels," *Neuromodulation*, vol. 20, no. 7, pp. 690-702, 2017.

[13] Cardiva. (24 May 2018). *AXIUM Implantable system for neurostimulation of the dorsal root ganglia*. Available: https://cardiva.com/productos/axium-2-2/?lang=en

[14] *Axium manual*. Available: https://www.accessdata.fda.gov/cdrh_docs/pdf15/P150004d.pdf

[15] Avid. (11 Jun 18). *Avid Medical Inc. Catalog*. Available: http://www.i-ma.com/brochures/Avid%20Medical/Avid_Medical-Catalog.pdf

[16] T. R. Kucklick, *The medical device R&D handbook*. CRC Press, 2012.

[17] L. Santos-Carreras, M. Hagen, R. Gassert, and H. Bleuler, "Survey on Surgical Instrument Handle Design: Ergonomics and Acceptance," *Surgical Innovation*, vol. 19, no. 1, pp. 50-59, 2011.

[18] A. Ali, D. H. Plettenburg, and P. Breedveld, "Steerable Catheters in Cardiology: Classifying Steerability and Assessing Future Challenges," *IEEE Transactions on Biomedical Engineering*, vol. 63, no. 4, pp. 679-693, 2016.

[19] M. Scali, T. P. Pusch, P. Breedveld, and D. Dodou, "Needle-like instruments for steering through solid organs: A review of the scientific and patent literature," *Proceedings of the Institution of Mechanical Engineers, Part H: Journal of Engineering in Medicine*, vol. 231, no. 3, pp. 250-265, 2017.

[20] P. A. York, P. J. Swaney, H. B. Gilbert, and R. J. Webster, "A wrist for needle-sized surgical robots," in *2015 IEEE International Conference on Robotics and Automation (ICRA)*, 2015, pp. 1776-1781.

[21] Pattex. *Gold Original glue*. Available: http://www.pattex.nl/dhz/producten/secondelijmen/secondelijm-classic.html

[22] Swann-Norton. *Surgical scalpel blade no. 11*. Available: https://www.swann-morton.com/product/18.php

[23] EnvisionTec. *R5*. Available: https://envisiontec.com/wp-content/uploads/2016/09/MK-MTS-R5R11-V01-FN-EN.pdf

[24] Brabantia. *Vervangingsset touch bin-slotje - black #383809*. Available: https://www.brabantia.com/nl/slotje-touch-binr-vervangingsset-black/

[25] BIC. *BIC Intensity Gel Clic gelpen*. Available: https://www.pinkcube.nl/pennen-bedrukken/bic-pennen-bedrukken/bic-intensity-gel-clic-gelpen.html

[26] M. Nissan and I. Gilad, "Dimensions of human lumbar vertebrae in the sagittal plane," *Journal of Biomechanics*, vol. 19, no. 9, pp. 753-758, 1986.

[27] D. Robinson. (2018). *L3 lumbar vertebrae*. Available: https://grabcad.com/library/l3-lumbar-vertebra-1

Appendix A: Solidworks drawings

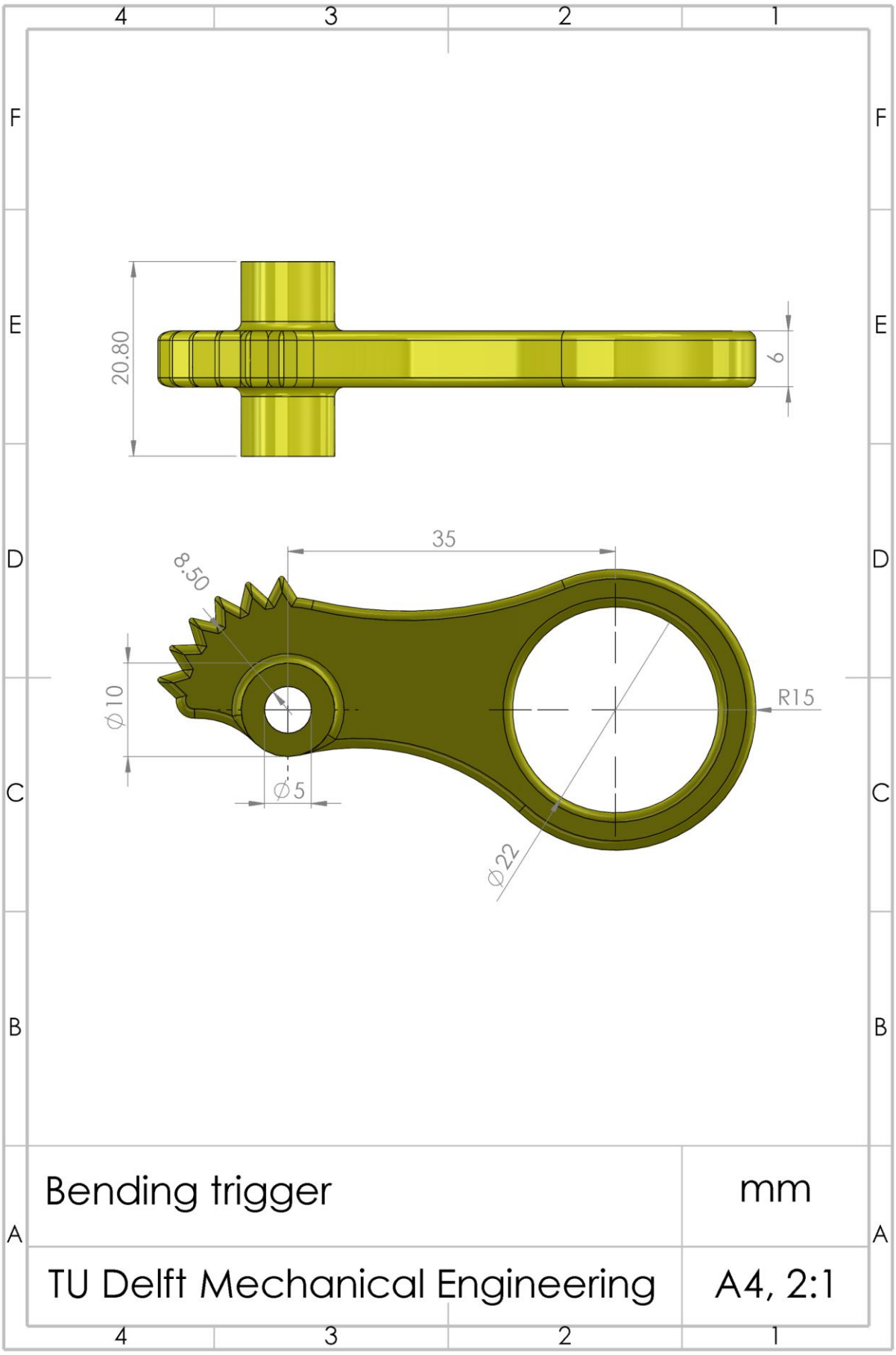

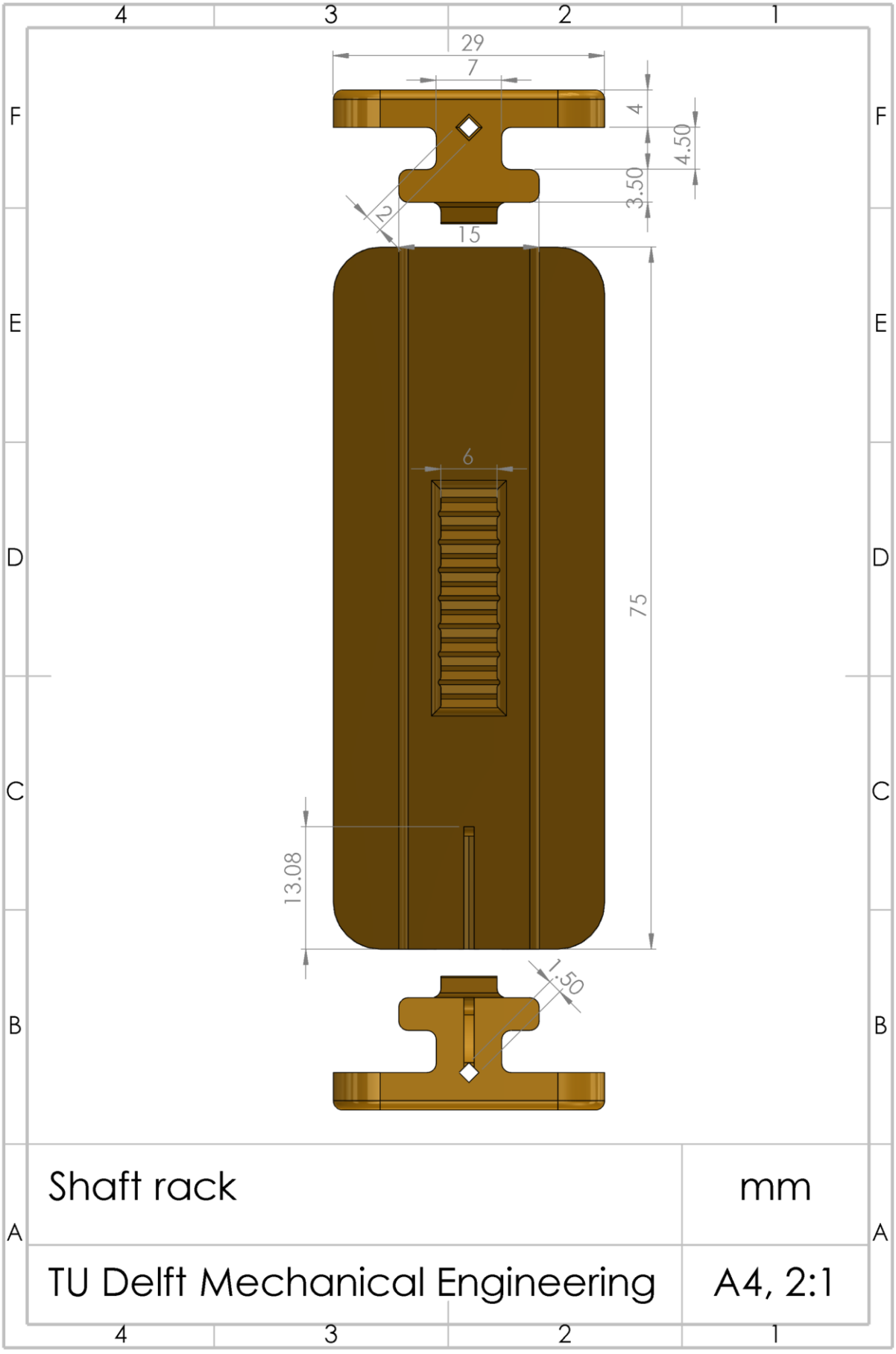
4
3
2
1
F
E
D
C
B
A
29
7
4
4.50
3.50
2
15
6
75
13.08
1.50
Shaft rack
mm
TU Delft Mechanical Engineering
A4, 2:1

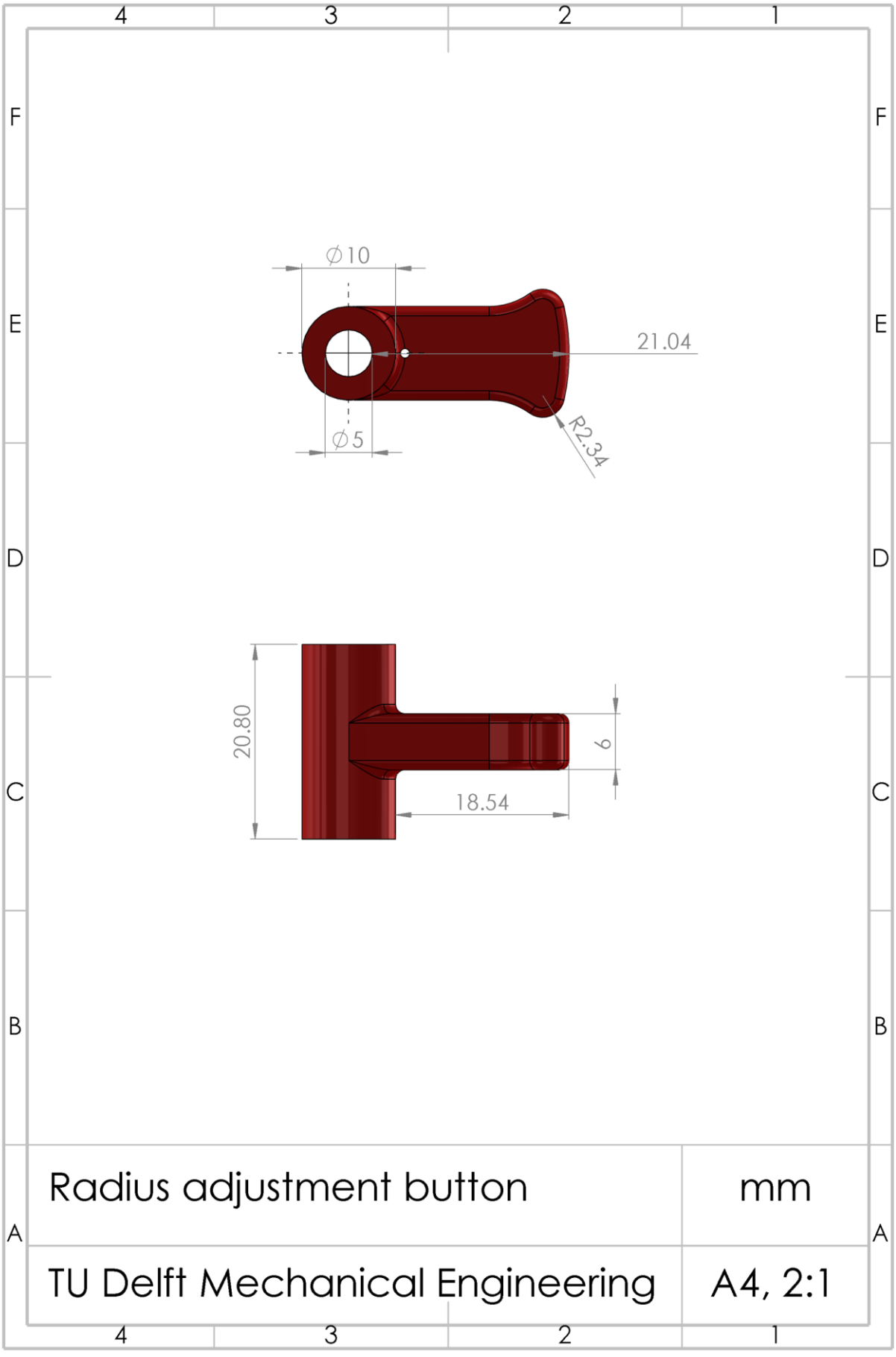
4
3
2
1
F
E
D
C
B
A
∅10
21.04
R2.34
∅5
20.80
6
18.54
Radius adjustment button
mm
TU Delft Mechanical Engineering
A4, 2:1

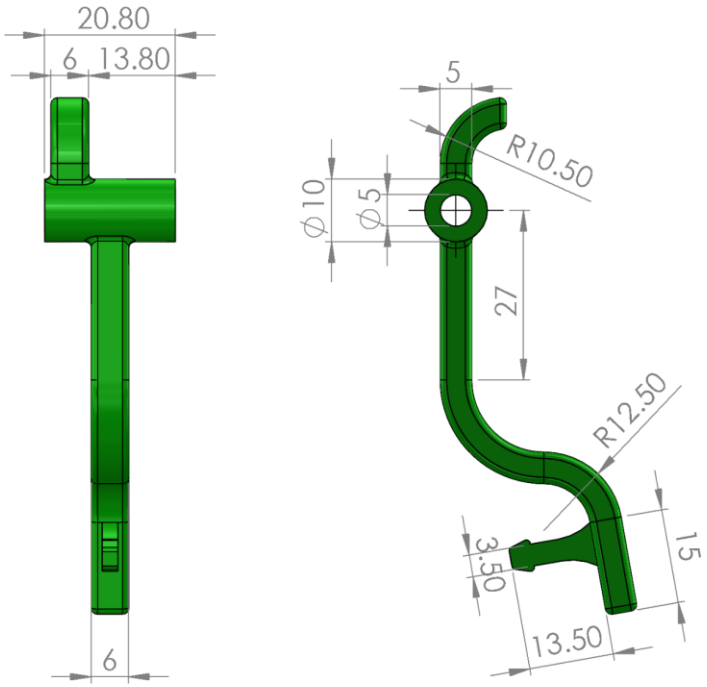

Catch lock bending trigger	mm
TU Delft Mechanical Engineering	A4, 1:1

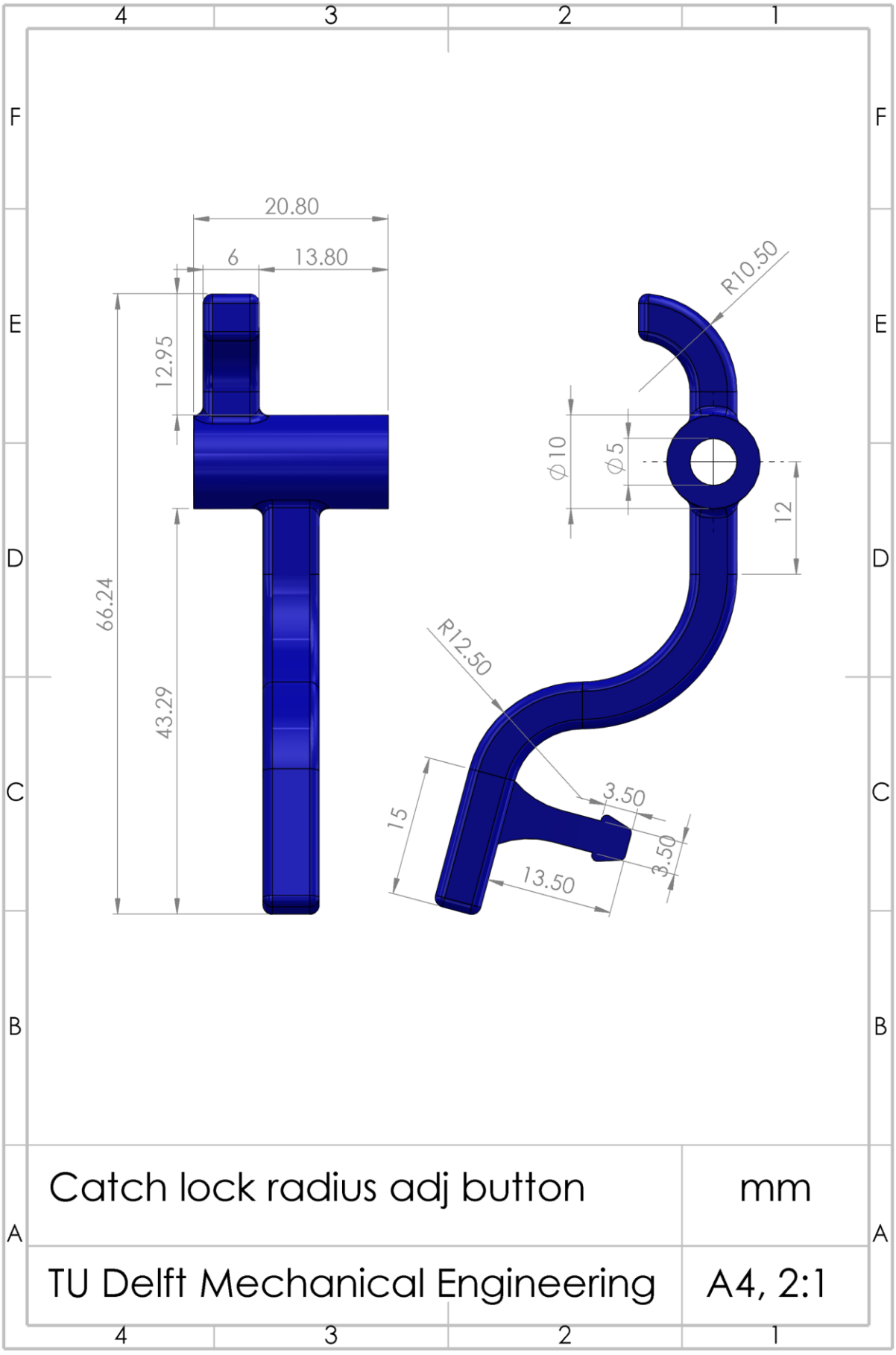
4
3
2
1
F
E
D
C
B
A
20.80
6
13.80
12.95
66.24
43.29
R10.50
ϕ10
ϕ5
12
R12.50
15
3.50
3.50
13.50
Catch lock radius adj button
mm
TU Delft Mechanical Engineering
A4, 2:1

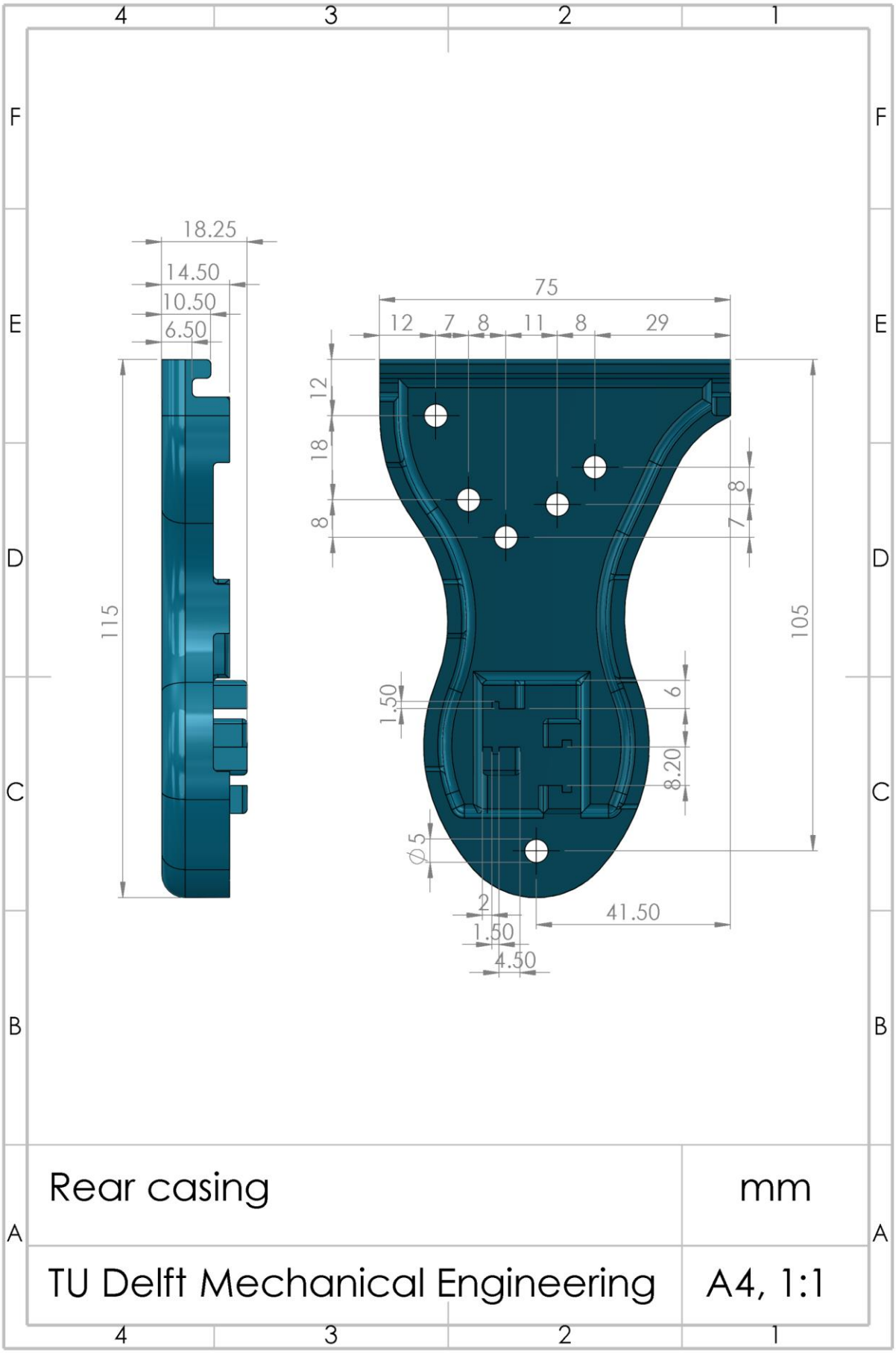
4
3
2
1
F
E
D
C
B
A
18.25
14.50
10.50
6.50
115
75
12
7
8
11
8
29
12
18
8
8
7
105
1.50
6
8.20
∅5
2
1.50
4.50
41.50
Rear casing
mm
TU Delft Mechanical Engineering
A4, 1:1

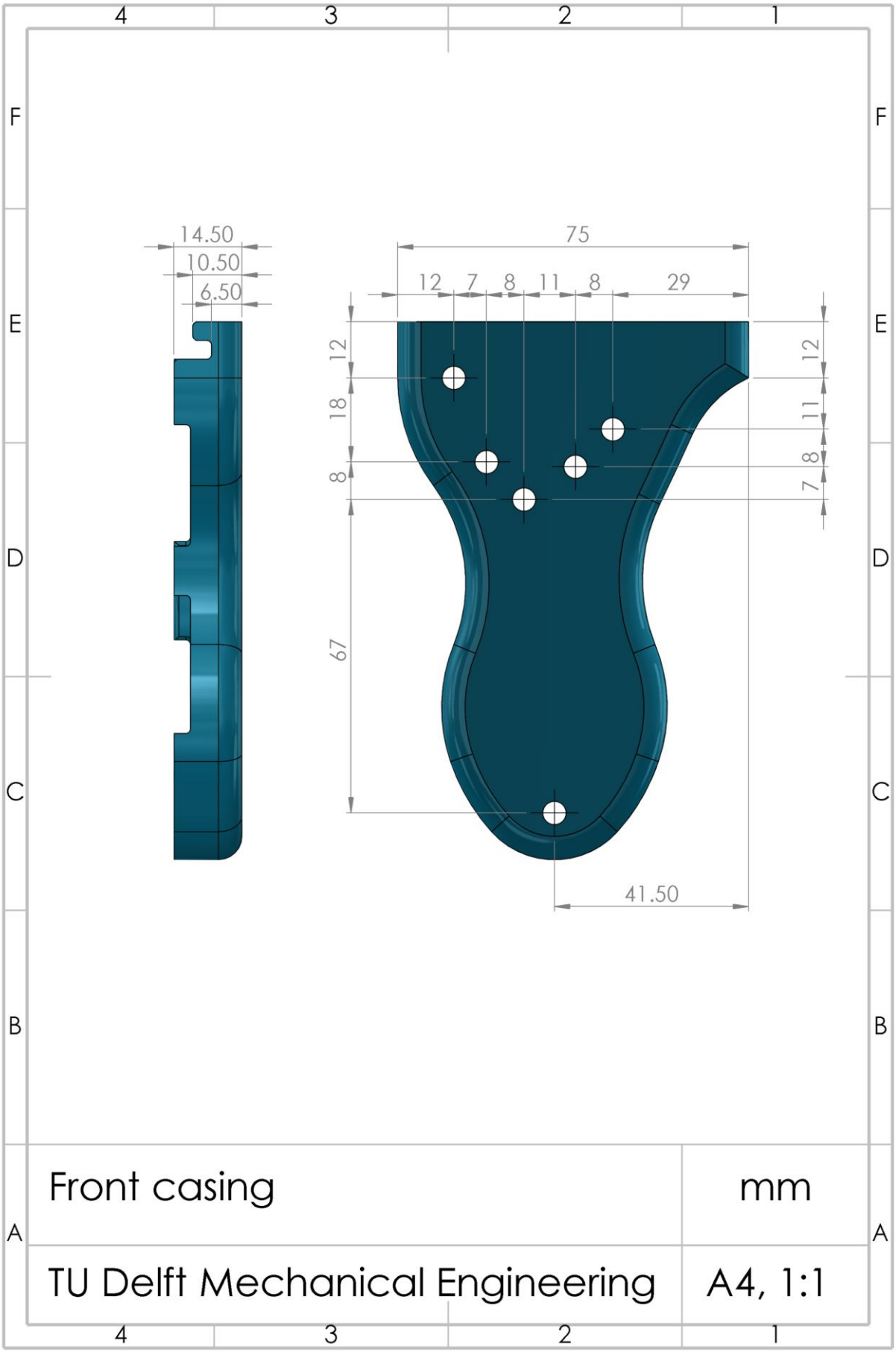
4
3
2
1
F
E
D
C
B
A
14.50
10.50
6.50
75
12
7
8
11
8
29
12
18
8
67
12
11
8
7
41.50
Front casing
mm
TU Delft Mechanical Engineering
A4, 1:1

Appendix B: Python calculations script

```
"""Calculate dimensions of the York et. al steerable tip design, the bending trigger and
the radius adjustment button."""

import math

# Constants
R_CURV_MIN = 3e-3  # Minimum radius of curvature (m)
R_CURV_MAX = 6.5e-3  # Maximum radius of curvature (m)

ANGLE_TRIGGER = math.radians(45)  # Maximum angle difference that the trigger can make
(deg)
ANGLE_RADADJ = math.radians(45)  # Maximum angle difference that the radius adjustment
button can make (deg)

N = 7  # Number of lateral slots in tip
G = 0.9e-3  # g parameter, see dimensions of slots (m)

R_O = 0.75e-3  # Outer radius of shaft (m)
R_I = 0.55e-3  # Inner radius of shaft (m)
R_CABLE = R_I - 0.05e-3  # Radius of cable when bending tip (m)

L_TIP = 20e-3  # Total tip length (m)

# Calculate slot dimension parameter y_
PHI_O = 2*math.acos((G-R_O)/R_I)
PHI_I = PHI_O/(2*math.acos((G-R_O)/R_O))

A_O = R_O**2*(PHI_O-math.sin(PHI_O))/2
A_I = R_I**2*(PHI_I-math.sin(PHI_I))/2

Y_O = (4*R_O*math.sin(PHI_O/2)**3)/(3*(PHI_O-math.sin(PHI_O)))
Y_I = (4*R_I*math.sin(PHI_I/2)**3)/(3*(PHI_I-math.sin(PHI_I)))

Y_ = (Y_O*A_O-Y_I*A_I)/(A_O-A_I)

def cablelengthdiff(r_curv, printmax=False, printmin=False):
    '''Calculate maximum angle of curvature, slot dimensions
    and cable length difference in tip when bending'''
    h = ((L_TIP-2*1.0e-3)/N)/(1+(r_curv-R_O)/(R_O+Y_))
    angle_curv = h*N/(R_O+Y_)
    c = (r_curv-R_O)*angle_curv/(N-1)

    l_cable = L_TIP-(r_curv-R_CABLE)*angle_curv

    if printmax:
        print('Slot dimensions: n = {}, g = {} mm, h = {} mm, c = {} mm'
              .format(N, G*1e3, h*1e3, c*1e3))
        print('Maximum angle of curvature: {} degrees'.format(math.degrees(angle_curv)))

    if printmin:
```

```
        print('Minimum angle of curvature: {} degrees'.format(math.degrees(angle_curv)))

    return l_cable


# Calculate minimum and maximum cable length difference
L_CABLE_MAX = cablelengthdiff(R_CURV_MIN, True, False)
L_CABLE_MIN = cablelengthdiff(R_CURV_MAX, False, True)

print('Minimum cable length difference: {} mm'.format(L_CABLE_MIN*1e3))
print('Maximum cable length difference: {} mm'.format(L_CABLE_MAX*1e3))

# Calculate radius of gear attached to trigger
R_TRIGGER = (L_CABLE_MAX)/ANGLE_TRIGGER

print('Trigger gear radius: {} mm'.format(R_TRIGGER*1e3))

# Calculate radius adjustment button cable length difference and cablehole radius
L_CABLE_DIFF = L_CABLE_MAX - L_CABLE_MIN
R_RADADJ = L_CABLE_DIFF/(ANGLE_RADADJ*math.sin(ANGLE_RADADJ))

print('Radius adjustment button cable length difference: {} mm'.format(L_CABLE_DIFF*1e3))
print('Radius adjustment button cablehole radius: {} mm'.format(R_RADADJ*1e3))
```